

A pathway analysis method for quantifying the contributions of precipitation and potential evapotranspiration anomalies to soil moisture drought

Chengyun Wang[a], Jie Chen[a,*], Lei Gu[b], , Guiyang Wu[a], Shanlin Tong[a], Lihua Xiong[a], Chong-Yu Xu[c,*]

[a] State Key Laboratory of Water Resources and Hydropower Engineering Science, Wuhan University, Wuhan, 430072, Peoples R China

[b] School of Civil and Hydraulic Engineering, Huazhong University of Science and Technology, Wuhan, 430074, Peoples R China

[c] Department of Geosciences, University of Oslo, Oslo, N-0316, Norway

[*] Correspondence to: Jie Chen (jiechen@whu.edu.cn); Chong-Yu Xu (c.y.xu@geo.uio.no)

Abstract:

Soil moisture drought, as one of the most important drought categories, is determined by both water supply (e.g., precipitation) and demand (e.g., potential evapotranspiration). To shed light on the underlying mechanisms driving soil moisture drought, the statistical multiple linear regression, machine learning, and modeling experiments methods have been pervasively used in early studies. However, these methods neglect the collinearity and interactions of climate variables, and thus cannot reflect the direct and indirect interaction of factors leading to soil moisture drought. To reveal the synergistic effects of water supply and demand on soil moisture drought, this study quantified the contributions of key drivers to the change of soil moisture drought by a path analysis method to exhibit the relationships between atmospheric movement state and soil moisture drought. Prior to applying the systematic path analysis model, we identified the spatial patterns of soil moisture droughts at different depths by using a state-of-art three-dimensional drought recognition method in the mainland of China. Our results showed that precipitation deficits dominated the interannual variation of soil moisture drought while increasing potential evapotranspiration only had marginal intensification in drought. The response of soil moisture drought to potential evapotranspiration was magnified by drought deterioration, especially in basically severe drought conditions. The total column water vapor and the horizontal divergence of the vapor flux, as well as temperature, directly affected precipitation and potential evapotranspiration and led to soil moisture drought through various direct and indirect processes. This study highlighted that the interactions among precipitation, potential evapotranspiration, and atmospheric vapor movement state in space and time were important for understanding the drought development mechanisms.

Keywords

Soil moisture drought; Drought severity; Standardized soil moisture index; Path analysis

1. Introduction

Drought is one of the most serious natural disasters with complex origins, perennial occurrence, and severe destruction (Wilhite et al., 2000). The deterioration of drought severity disturbs the biodiversity conservation of the natural ecosystem and the sustainable development of the social economy (Gu et al., 2020a; Kreibich et al., 2022). Drought is typically defined as a long-term imbalance in the water budget or between supply and demand, and can occur in all compartments of the hydrological cycle (Van Loon, 2015). Generally, drought is categorized into meteorological (atmosphere), hydrological (streamflow and groundwater), agricultural (soil moisture), and socioeconomic (human) types (Gu et al., 2020b; Heim, 2002; Wu et al., 2022). Agricultural drought is one of the most critical hazards, which is commonly defined as a deficit in soil moisture that affects plant growth or crop yields (Hong et al., 2021; Zhang et al., 2021b). Therefore, soil moisture has been widely used to evaluate agricultural drought conditions (Cai et al., 2021; Deng et al., 2021; Narasimhan and Srinivasan, 2005).

Even though soil moisture drought has multiple natural properties (Manning et al., 2018), it usually can be seen as the result of the imbalance of precipitation and potential evapotranspiration affected by the energy budget and water cycle of the land-atmosphere coupling system. The water supply (precipitation), which can alleviate soil moisture drought, has spatial heterogeneity in the land-atmosphere system, and its variation is mostly influenced by the water vapor movement (He et al., 2022; Liu et al., 2017). Many studies investigated the response mechanism of soil moisture drought to the changes in precipitation and potential evapotranspiration (Cheng and Huang, 2016; Luo et al., 2017; Song et al., 2020; Wang et al., 2018). It is also widely accepted that the changing temperature promotes soil moisture drought indirectly by increasing potential evapotranspiration

(Stefanon et al., 2014).

Statistical multiple linear regression methods, machine learning, and modeling experiments with control variables are usually used to investigate the complex interrelationships between water supply and demand for soil moisture drought in previous studies. For example, Bai et al. (2019) used multiple linear regression to calculate the rate of contribution of precipitation and temperature to soil moisture changes in the Tibetan Plateau and found that precipitation is the dominant factor compared to the temperature. Zhang et al. (2022) used various explainable machine learning methods to simulate flash soil moisture drought over China by considering the multiple meteorological variables in the adjacent time to drought onset and found that the lack of precipitation and the increase of evaporation demand have different effects on drought in different regions. Luo et al. (2017) used a set of modeling experiments controlling for different climate variables to analyze the reason for the multiyear agricultural drought in California and revealed that precipitation deficits are largely responsible for the agricultural drought.

However, due to the nonlinear and collinearity problems among climate factors, the number of independent variables used for drought analysis was limited and varied from partition to partition, especially for the multiple linear regression methods (Liu et al., 2022). Although machine learning and modeling experiments can interpret all the drivers' contributions and achieve good performance in constructing nonlinear interactions among variables, machine learning cannot quantify the effect of a factor alone, and neither of them considers the role of interactions among climate factors in soil moisture drought. Moreover, the response mechanisms of soil moisture are complex with both direct and indirect factors. In previous studies, the impacts of various climatic factors on the development of soil moisture drought were evaluated from the perspective of direct impacts, while how certain factors directly or indirectly affect the development of soil moisture drought simultaneously still remains poorly understood (Nemergut et al., 2011; Waldrop et al., 2017).

Path analysis is a specific technique for analyzing conceptual models by quantifying the relationships and interactions between networks of factors, which allows simultaneous analysis of multiple direct and indirect relationships among variables and can solve covariance problems caused by correlations (Gui et al., 2017; Velayati et al., 2021). It is often referred to as causal analysis because it is used to test or confirm prior models based on empirical data (Keller et al., 2022). Path analysis has the advantage of simultaneously assessing all relevant trajectories, accounting for the role of independent and/or dependent mediators in outcome development (Devlieger and Rosseel, 2017). Many studies used path analysis in psychology, business economics, and mathematics to reveal the complex relationships of the variables that affected them (Bennett et al., 2020; Zhang et al., 2015). Due to the simplicity of its underlying statistical theory and its potential to solve important substantive problems, it is also used by many ecologists in the attribution analysis of agricultural land use and soil ecological change (A et al., 2019; Keller et al., 2022). Therefore, as a primary method of attribution analysis, path analysis has a great potential to analyze the mechanisms of direct and indirect effects of individual variables on soil water drought in complex environments. However, to the best of our knowledge, this method has not been used to quantify the contributions of climate variables to soil moisture drought.

Accordingly, this study proposes, for the first time, the use of the path analysis method to investigate the direct and indirect relationships between driving factors and soil moisture drought. Specifically, the path analysis model is constructed to quantify the impact of demand and supply on soil moisture drought from the perspective of the atmospheric water cycle to advance our understanding of the water supply and demand for soil moisture drought. The main factors of atmospheric water vapor change (e.g., the total column water vapor, TCWV, and the horizontal divergence of the vapor flux, DIVQ) and temperature were used as the extrinsic climatic forcing factors that indirectly affect soil moisture. The precipitation and potential evapotranspiration are considered to be factors directly affecting soil moisture drought.

2. Dataset and study area

2.1 Study area

This study quantified the contribution of precipitation and potential evapotranspiration anomalies to soil moisture drought in the mainland of China. China is located in East Asia and borders the Pacific Ocean, spanning from 3°N to 54°N and from 73°E to 135°E (Wu et al., 2020), covering an area of 9.6×10^6 km^2. To analyze the soil moisture drought characteristics over different climate regimes, four subregions were defined based on the multi-year average aridity index (AI = precipitation / potential evapotranspiration) for the 1950-2021 period (Huang et al., 2014; Liu et al., 2018; Xu et al., 2019). The four subregions consist of Arid (AI< 0.2), Sub-Arid ($0.2\leqslant AI < 0.5$), Sub-Humid ($0.5\leqslant AI<0.65$), and Humid ($AI\geqslant0.65$).

2.2 ERA5 data

This study used the fifth generation of European Reanalysis (ERA5) data to characterize the drought. ERA5 is the latest reanalysis product from the European Centre for Medium-Range Weather Forecasts (ECMWF). It covers the period from 1950 to the present and is updated daily with a latency of five days (Viggiano et al., 2021; Yang et al., 2021). The product is produced using

4D-Var data and the latest European Medium-range Weather Forecast model (CY41R2) that was operational in 2016, combining many historical observations including ozone, aircraft, and surface pressure, new decommissioning and a variety of the latest data sets and instruments. ERA5 is one of the most widely used reanalysis datasets for the study of soil moisture due to its good adaptability and high spatial and temporal resolutions (Ling et al., 2021; Zhang et al., 2021b). The used variables in this study included monthly precipitation, temperature, potential evapotranspiration, total column water vapor, the horizontal divergence of the vapor flux, and three layers of soil moisture (including 0–7 cm, 7–28 cm, and 28–100 cm) for the 1950-2021 period, with a spatial resolution of 0.25°.

2.3 In situ datasets

The in-situ soil moisture data were used to evaluate the performance of ERA5 in simulating soil moisture, which were downloaded from the National Meteorological Information Center of China (CMA) (http://cdc.cma.gov.cn/home.do). The data have been collected from 778 agricultural-meteorological stations, covering the period from 1991 to 2013, with a temporal resolution of every 10 days (on days 8, 18, and 28 of each month) (An et al., 2016). This dataset contains soil relative humidity for 10 cm, 20 cm, 50 cm, 70 cm, and 100 cm. The distribution of stations is shown in Fig.1.

Since the in-situ soil moisture data are relative value (θ; %), while ERA5 simulations are soil volumetric water contents (θ_v; m^3 m^{-3}), the observed data were transformed to the same form of ERA5 data by the following equation:

$$\boldsymbol{\theta_v} = \boldsymbol{\theta} \cdot \boldsymbol{\theta_f} \cdot \boldsymbol{\rho_b} \qquad (1)$$

where θ_f is the field capacity, and ρ_b is the dry bulk density. The in-situ field capacity and dry bulk density data set were obtained from the National Meteorological Information Center of the China

Meteorological Administration (http://cdc.cma.gov.cn/home.do) for the 1981-1998 period.

To compare ERA5 data with observed data at different depths, the soil volumetric water content obtained by ERA5 was calculated by taking the soil thickness as the weighting coefficient to obtain the corresponding soil volumetric water content for 0-10 cm, 10-20 cm, 20-50 cm, and 50-70 cm. Due to the poorer quality of the observed data for other seasons, only soil moisture in summer (June–August) was used to evaluate the ERA5 data.

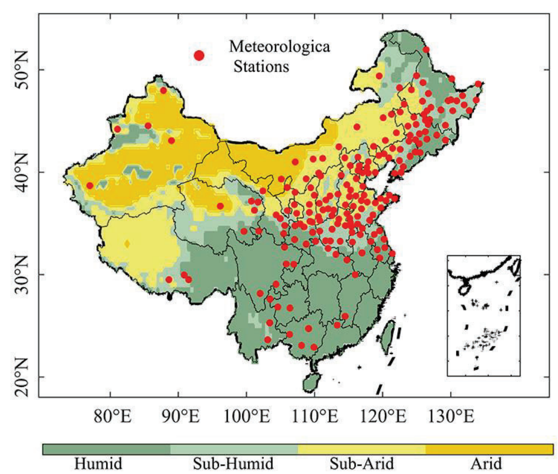

Fig.1 Distribution of soil moisture observation stations in China

3. Methods

3.1 Soil moisture drought identification

Standardized soil moisture index (SSI) is one of the most straightforward indices developed and validated in many studies to monitor agricultural droughts (Afshar et al., 2022; Mpelasoka et al., 2008). In this study, SSI was estimated as a standardized anomaly for the 1950-2021 period. The negative value of SSI indicates that soil moisture is lower than the average level during the study period, which is used to characterize the degree of drought. Grids with SSI < -1 were used in this study for drought recognition.

The soil moisture droughts were identified using a spatial identification procedure, which was based on a clustering algorithm that incorporates spatial contiguity (Andreadis et al., 2005; Lloyd-Hughes, 2012), from a three-dimensional perspective (longitude, latitude, and time). The three-dimensional drought can be expressed by DI ($n_{lon} \times n_{lat} \times n_t$), where n_{lon} and n_{lat} are the number of girds along longitude and latitude, respectively, and n_t is the number of months along time dimension (Xu et al., 2015). The recognition processes of drought events include the following three steps:

Step 1: Identifying drought patches. For each moment, we set a minimum drought index threshold SSI (-1.0 in this study) to identify the drought state of each grid, considering spatial continuity. Then we cluster the grids with the value of index less than -1 into several drought patches to obtain patch numbering matrix L.

Step 2: Determining the connection of drought patches on two adjacent months. We first determine a minimum drought patch area A_o, and the drought patches which are smaller than this threshold will be omitted.

The threshold A_o is an important parameter in this three-dimensional method. A_o is a function of the total number of droughts and the duration of droughts, which determines the spatiotemporal behaviors of drought patches. It depends also on the size of study area. Based on a sensitivity test, Wang et al. (2011) suggested a minimum drought patch area of 150000 km^2 (approximately 1.5% of the study area) for China. Liu et al. (2019), and Zhu et al. (2019) also used a similar criterion (equivalent to 1.5% of the study area) to analyze droughts in their study areas. In our study, the same threshold standard, 150000 km^2 was employed as the minimum drought patch area.

As shown in Fig.S1, considering the two adjacent months, *t*, and *t*-1, if any couples of patches (denoted by E_{t-1} and E_t) between the two months have an overlap area larger than A_o, E_{t-1} and E_t belong to the same drought event, otherwise, they are different drought events.

Step 3: Identifying drought events. Repeated Step 2 until the last period (from the second month of the 72 years to the last month). Finally, all the drought patches with spatio-temporal continuity are assigned a unique number, that is, three-dimensional drought events.

Four parameters are calculated to describe the determined drought events. They are defined as follows:

(1) Duration (D) is the duration of a drought event, calculated as the time interval between the start and end of a drought event.

(2) Severity (S) is an expression of water shortage, indicating the total amount of water on a spatio-temporal scale that is needed to recover back to normal conditions. The severity of the drought event (taking the E^{th} as an example) is defined as:

$$\boldsymbol{S_E} = \sum_{\boldsymbol{t=1}}^{\boldsymbol{NT}} \left(\sum_{\boldsymbol{j=1}}^{\boldsymbol{N}} \boldsymbol{area_{t,j}} \cdot \boldsymbol{DI_{t,j}} \right) \qquad (2)$$

where S_E is the severity of the E^{th} drought event (km^2 month), S is the severity the of voxels (km^2 month), NT and N are the duration and the number of covering grids of the three-dimensional precipitation event. $area_{t,j}$ is the area of grids.

In the attribution section, we defaulted the area of each grid point to one unit according to the method of Yan et al. (2018).

(3) Affected Area (A) is the area swept by a drought event. It is a region projected onto the surface of latitude and longitude in a three-dimensional space-time domain.

(4) Centroid (C) is the center of the drought event, which represents the position of the drought

event in three-dimensional space-time (longitude, latitude, and time).

3.2 Influence factors analysis for drought events

3.2.1 Path Analytic Method

The sensitivity of soil moisture drought to precipitation, potential evapotranspiration, and other possible drivers was estimated using path analysis from the perspective of correlation. Before using the path analysis, we first standardized potential evapotranspiration, precipitation, TCWV, divQ, temperature with z-scores. The structural model was based on areas where three-dimensional soil moisture drought occurred (Fig.2). To perform path analysis, the variables were divided into three main categories: input, intermediate, and output (Ebrahimi et al., 2021), with TCWV, temperature, and divQ used as input variables. Although many studies have found that atmospheric water vapor movement and temperature strongly influence soil moisture drought, they do not cause such changes by themselves. Potential evapotranspiration and precipitation were assumed to directly affect SSI, and the TCWV, divQ, and temperature indirectly affect SSI through them.

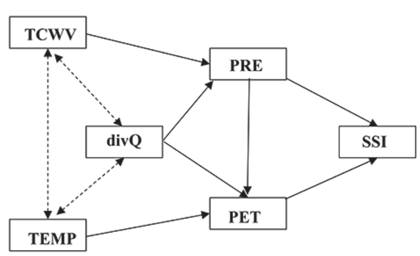

Fig.2 Path diagram for SSI and possible drivers. Arrows connect exogenous and endogenous variables, called paths. The direction of the path indicated by the single-headed arrow is determined by the causal relationship between exogenous and endogenous variables. The double-headed arrow indicates a correlation between TCWV, temperature (TEMP), and divQ but not causality. TCWV, temperature, and divQ are the input variables that affect the SSI indirectly. In particular, TCWV and divQ affect SSI by affecting precipitation (PRE) and potential evapotranspiration (PET), and temperature affect SSI by affecting potential evapotranspiration, where precipitation and potential evapotranspiration directly affect the SSI.

We calculated the standardized total effects of input and intermediate properties on the SSI to show the relative effects of water supply and demand factors, atmospheric water vapor movement, and temperature on SSI change. We also calculated the standardized effects of atmospheric water vapor movement and temperature on precipitation and potential evapotranspiration in different pathways to show the relative importance of different pathways in mediating climate variables change on SSI. All path analyses were conducted using package *lavaan* in R 4.0.5 (Hou et al., 2018; Rosseel, 2012).

3.2.2 Quantile regression

Under different severity of drought, the influence mechanisms are various. In order to further analyze the influence of precipitation and potential evapotranspiration on different degrees of drought, especially extreme drought, we used a quantile regression model proposed by Koenker and Bassett (1978) to measure the impact of different quantiles of drought on precipitation and potential evapotranspiration. Compared with conventional linear regression, quantile regression is less affected by outliers, which can better analyze the influence of explanatory variables on the conditional distribution of explanatory variables in different quantiles (Chen et al., 2019).

Quantile regression is regarded as an extension of least squares regression, which not only yields a regression to the mean but also provides a statistical way to express the change in the percentile of the data. Let y be a continuous random variable with cumulative distribution function $F(y)$, the τ quantile function of y is defined as $Q\ (\tau)$, such that P $[y \leq Q(\tau)] = \tau$. For the quantile τ, the quantile regression can be written as:

$$\boldsymbol{Y} = \boldsymbol{X}'\boldsymbol{\beta}_{\boldsymbol{\tau}} + \boldsymbol{\varepsilon}_{\boldsymbol{\tau}} \qquad (3)$$

where Y=(y_1, y_2, …, y_k)^T represents the explained variable (in our study the monthly total SSI) in the model, X=(1,x_1, x_2, …, x_k)^T is the explanatory variable (in our study the monthly total precipitation and monthly total potential evapotranspiration), β_τ =(β_0 , β_1 ,…, β_k) is the parameter vector, ε_τ= ($\varepsilon_{1\tau}$, $\varepsilon_{2\tau}$, …, $\varepsilon_{k\tau}$)^T is the error vector, ($0 < \tau < 1$) represents a specific quantile, and the estimated parameter is mainly calculated by weighted residuals and minimum values.

In this study, the explanatory variables (monthly total precipitation and monthly total potential evapotranspiration) are standardized by z-scores to have zero-mean and unit standard deviation. This type of standardization allows us to quantify the impact of one-unit standard deviation on the regression in the explained variable, which makes it feasible to compare the relative importance of each variable.

4. Results

4.1 ERA5 soil moisture evaluation

The gauged soil moisture at different depths is adopted to verify that obtained from ERA5. The spatial patterns of the 22-year (1992-2011) averaged soil moisture for the observations and ERA5 product at four different soil layer depths were analyzed during June-August (JJA) (Fig.3). The observed soil moisture, which is considered real soil moisture data, is larger in Northeast and Southwest China, and smaller in Northwest China at four depths. The observed soil moisture values decrease from southeast to northwest. Generally, ERA5 can capture the overall spatial distribution of the observed soil moisture at the four different depths. ERA5 shows positive biases for drier regions and negative biases for wetter regions. Since the observed data are too limited, especially for southern and northwestern China, this comparison is only used to get a rough insight into the similar spatial pattern of ERA5 and gauged soil moisture data. The ERA5 data have been widely used in China to investigate soil moisture drought (Zhang et al., 2021a).

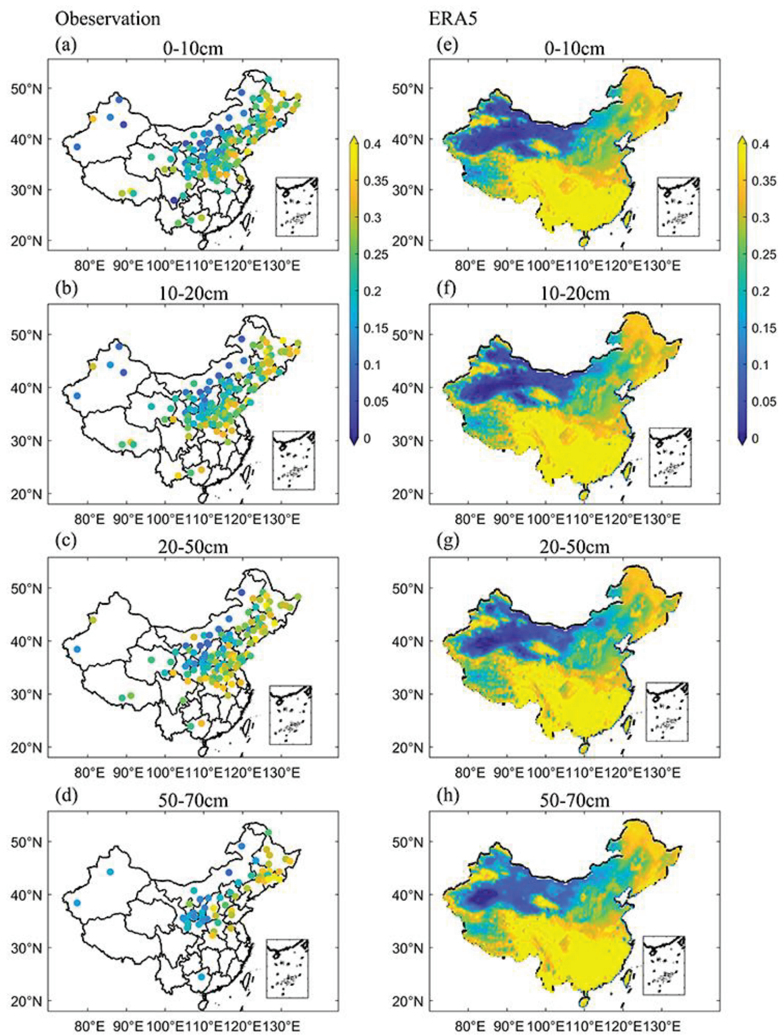

Fig.3 Spatial distributions of annual averages of observations (a-b) and ERA5 (e-f) soil moisture at different depths (m^3m^{-3} volumetric moisture content) during JJA for the period of 1992-2011 in China

We then investigate the temporal correlation of soil moisture between observations and ERA5 (Fig. 4). Generally, the temporal correlation is reasonably good between observed and ERA5 data in Northeast, North, and Northwest China, with correlation coefficients being higher than 0.5. And the stations with high correlation and passing the significance test ($p<0.1$) are distributed all over the country, which is consistent with Li et al (2021). The significant correlations are found on 27%, 23.66%, 20.51%, and 16.67% of the stations with correlation coefficients larger than 0.45, 0.44, 0.43, 0.46 at 0-10cm, 10-20cm, 20-50cm, and 50-70cm depths, respectively. With the deepening of soil layer depths, the correlation coefficient shows a downward trend. Overall, it can be concluded that the ERA5 can capture the spatial and temporal distribution characteristics of observed soil moisture at different depths in China.

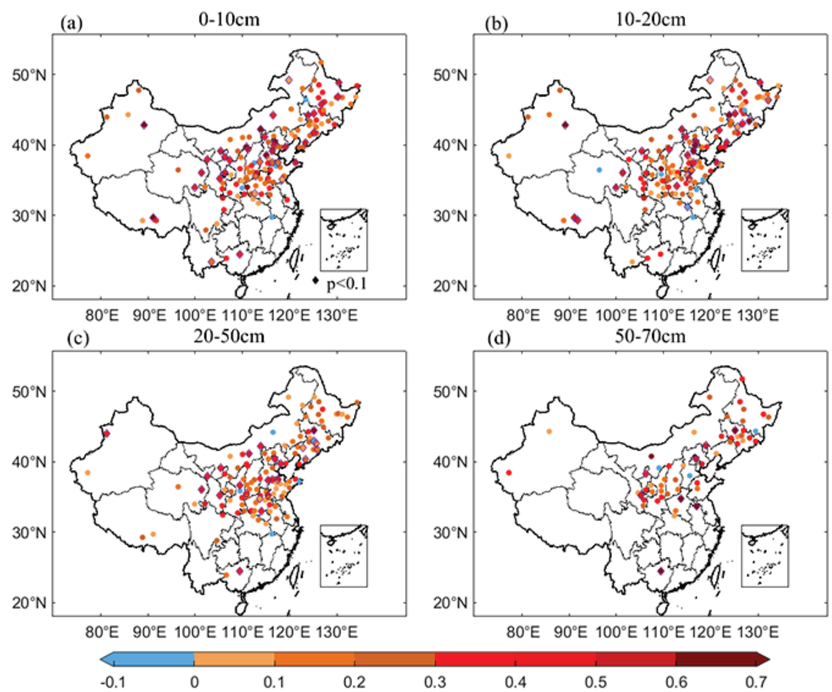

Fig.4 Correlation coefficient between ERA5 and measured soil moisture at different depths during JJA for the period of 1992-2011 in China (P<0.1, P means the significant level)

4.2 Spatial variation of soil moisture droughts at different depths

Fig.5 plots the spatial distribution of all drought centroids at different depths. Here, circles of different colors represent different durations while circles of various sizes represent varying severities during 1950-2021. Soil moisture droughts with greater severity and longer duration at 0-10 cm soil layer depth mainly cluster over Northwest, North, and Central China than other regions (Fig.5a). Generally, the distribution patterns of drought event severities at 0-20cm, 0-50 cm, and 0-

70cm depths are similar to that at the depth of 0-10 cm. However, with the increase of soil layer depth, the total drought count decreases while drought duration increases. In total, 661, 614, 529, and 462 droughts events were identified at 0-10cm, 0-20cm, 0-50cm, and 0-70cm, respectively. Of those, the durations of 116 (17.5%), 119 (19.4%), 130 (24.6%), and 121 (26.2%) droughts are longer than 3 months at four depths, which indicates the proportion of long-duration droughts is greater when the soil layer is deeper.

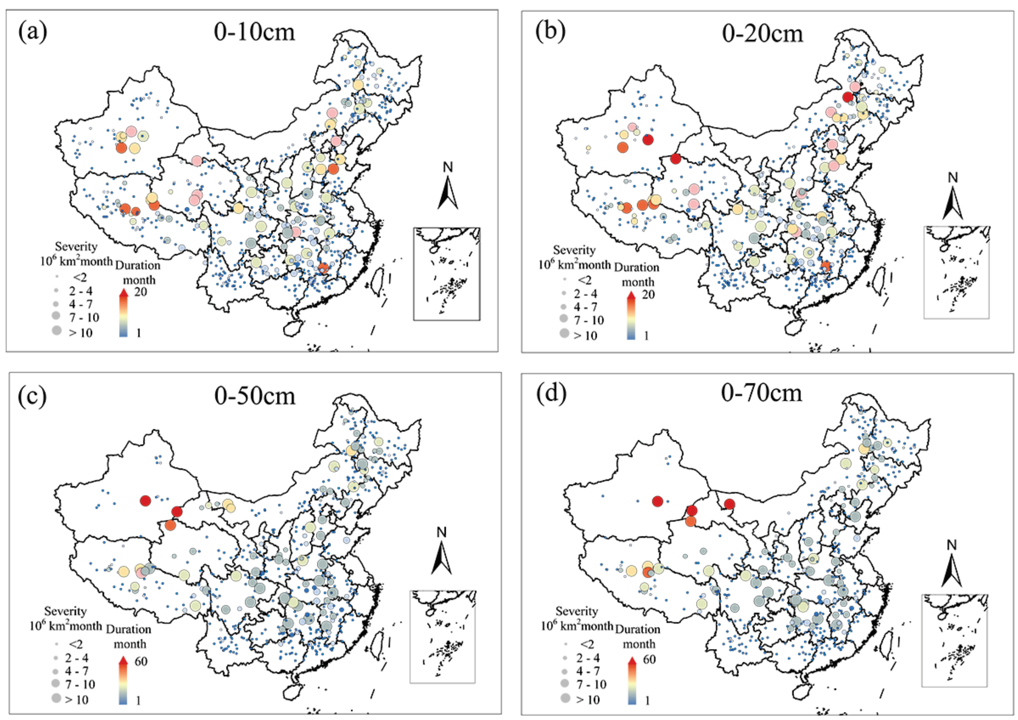

Fig. 5 Spatial distribution of soil moisture drought events during 1950-2021.

4.3 Impacts of precipitation and potential evapotranspiration on droughts

4.3.1 Overall climate impacts on SSI at different depths

Soil moisture drought is affected by a changing and interacting set of extrinsic climatic forcing factors and hydrological properties. We select four different soil layer depths to show the driving factors response to soil moisture droughts at different soil layer depths over China (Fig.6). The path analysis models are considered acceptable according to Table.S1. The water supply and demand can well explain the change in SSI. The direct effect of precipitation on SSI is consistently positive and larger than the negative direct effect of potential evapotranspiration on SSI at different depths, which means precipitation deficits dominate the interannual variation of soil moisture drought with standardized path coefficients larger than 0.7. However, with the increase of the depth, the variance explanation rate (R^2) of precipitation and potential evapotranspiration for soil moisture drought decreases, which indicates that there are other hydrological factors, such as runoff, that affected soil moisture drought. For 0-10cm soil moisture drought, precipitation, and potential evapotranspiration explain 77.7% of the change in SSI, while for 0-20cm, 0-50cm, and 0-70cm, the values are 73.2%, 63.2%, and 56.7%.

TCWV negatively affects soil moisture drought by having a positive effect on precipitation and a negative effect on potential evapotranspiration. Moreover, divQ positively affects soil moisture drought through the enhancement of potential evapotranspiration and attenuation of precipitation. Temperature exacerbates drought by intensifying potential evapotranspiration. Some of the paths are not statistically significant owing to the calculation at the national scale, especially for deep soil layers. From 0-10cm to 0-70cm soil depth, the absolute value of the standardized potential evapotranspiration path coefficient decreases, mainly from 0.37 to 0.23. In addition, the effect of potential evapotranspiration on soil moisture drought is not significant at 0-50cm and 0-70cm, and so does the TCWV, divQ, and temperature. It indicates that at the depth of 0-50cm and 0-70cm, only precipitation has a statistically significant effect on soil moisture drought.

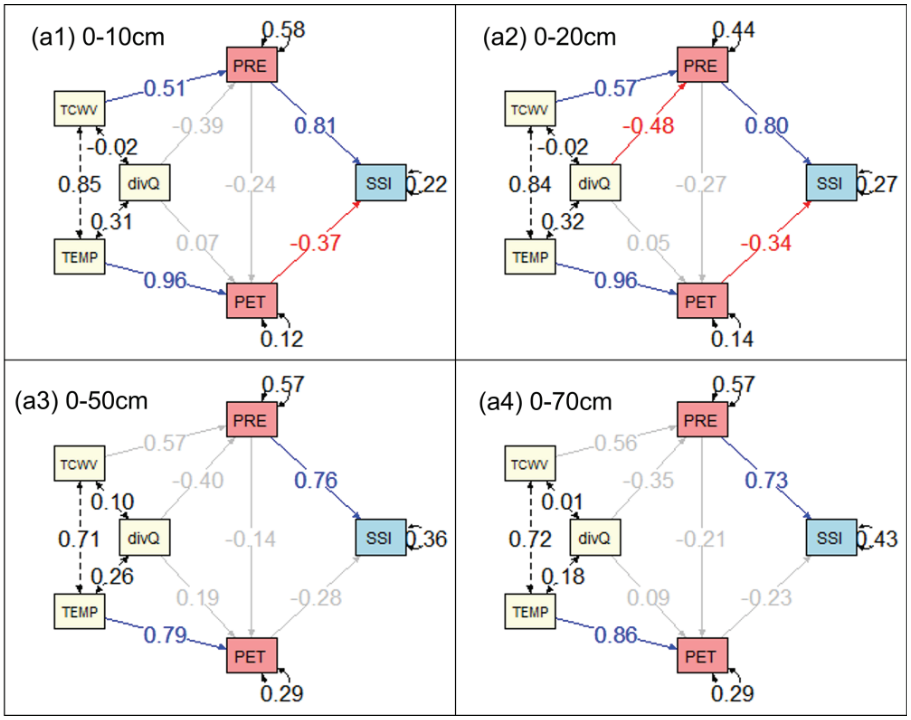

Fig.6 Path analysis of SSI at different depths (a1, 0-10cm; a2, 0-20cm; a3, 0-50cm; a4, 0-70cm). The arrow represents the effect path and direction, the blue and red arrows represent significant ($P<0.05$; P means the significant level) positive and negative effect paths, respectively, and the gray arrow represents the insignificant pathways. The number on the one-headed arrow is the standardized path coefficient. The black dashed doubled-headed arrow represents the simple correlation relationship between the two factors, and the number on it is the correlation coefficient. The values on PRE, PET, and SSI are the amount of explained variation (R^2) of the variable explained by all paths in the model.

4.3.2 Climate impacts on SSI in different regions

The path analysis results of soil moisture drought in different regions (Humid, Sub-Humid, Sub-Arid, and Arid) are presented in Fig.7. The model results show that precipitation and atmospheric vapor movement are the main influencing factors for soil moisture drought in different regions. However, the effects of atmospheric vapor movement and temperature on soil moisture drought are in contrast between humid and arid regions. In other words, the effects are more significant in humid regions than in arid regions. The number of insignificant pathways is increasing, mainly from 1 to 4, and the proportion of explained variation in precipitation decreases in these models, mainly from 90% to 45%, from the humid to the arid regions. In Humid, Sub-Humid, and Sub-Arid areas, precipitation positively affects soil moisture drought and potential evapotranspiration negatively affects soil moisture drought significantly, while in the Arid area, the effect of potential evapotranspiration on soil moisture drought is not significant. The negative effect of precipitation on soil moisture drought is gradually increasing from the humid area to the arid area, especially in the Arid region, where the effect of potential evapotranspiration on soil moisture drought is very small (Fig.S2).

By analyzing the range of the standardized direct effect of precipitation and potential evapotranspiration on soil moisture drought in different regions, we find that the effect changes smoothly for 0-50 and 0-70cm from humid to arid areas. While for 0-10 and 0-20cm, the effect shows a larger turnaround between Sub-Humid and Sub-Arid areas, mainly from 0.75 to 0.9. Shallow soil moisture drought has a rapid response to different climate anomaly patterns, while deep soil moisture drought has a strong persistence in the soil layer, and its response to climate anomaly needs a longer time to accumulate.

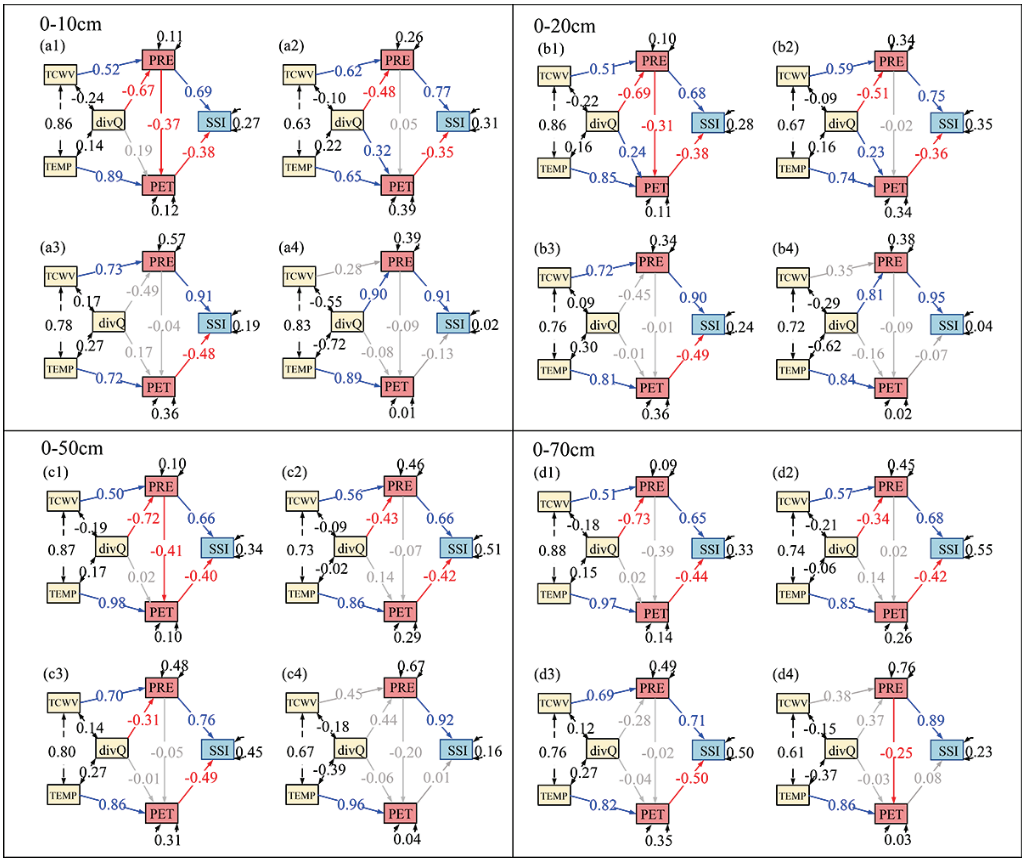

Fig.7 Path analysis of SSI in different regions (a1,0-10cm Humid; a2,0-20cm Humid; a3,0-50cm Humid; a4,0-70cm Humid; b1,0-10cm Sub-Humid; b2,0-20cm Sub-Humid; b3,0-50cm Sub-Humid; b4,0-70cm Sub-Humid; c1,0-10cm Sub-Arid; c2,0-20cm Sub-Arid; c3,0-50cm Sub-Arid; c4,0-70cm Sub-Arid; d1,0-10cm Arid; d2,0-20cm Arid; d3,0-50cm Arid; d4,0-70cm Arid)

4.3.3 Climate impacts on SSI at different seasons

After investigating the spatial patterns of driving mechanisms of soil moisture drought, we also probe into the temporal disciplines of the main mechanism of soil moisture drought (Fig. 8). We use 0-10cm drought for demonstration. For other depths, the seasonal effect pattern is similar to 0-10cm (Fig.S3). We do not analyze soil moisture drought in winter, due to freezing in northern and frigid zones, soil moisture shows little change. In addition, the seasonal path analysis in the Arid area is either not analyzed, because precipitation dominates the drought in the Arid area with standardized path coefficients larger than 0.89 at different depths (Section 4.3.1).

The results show that summer soil moisture drought is mainly dominated by potential evapotranspiration with a standardized effect of about -0.9, while spring and autumn droughts are mainly affected by the deficiency of precipitation. Further analysis shows that drought severity dominated by potential evapotranspiration is higher, while that dominated by precipitation is relatively lower. When drought occurs, lower soil moisture and higher temperature in summer contribute to the increase of potential evapotranspiration, which has an increasing impact on soil moisture drought.

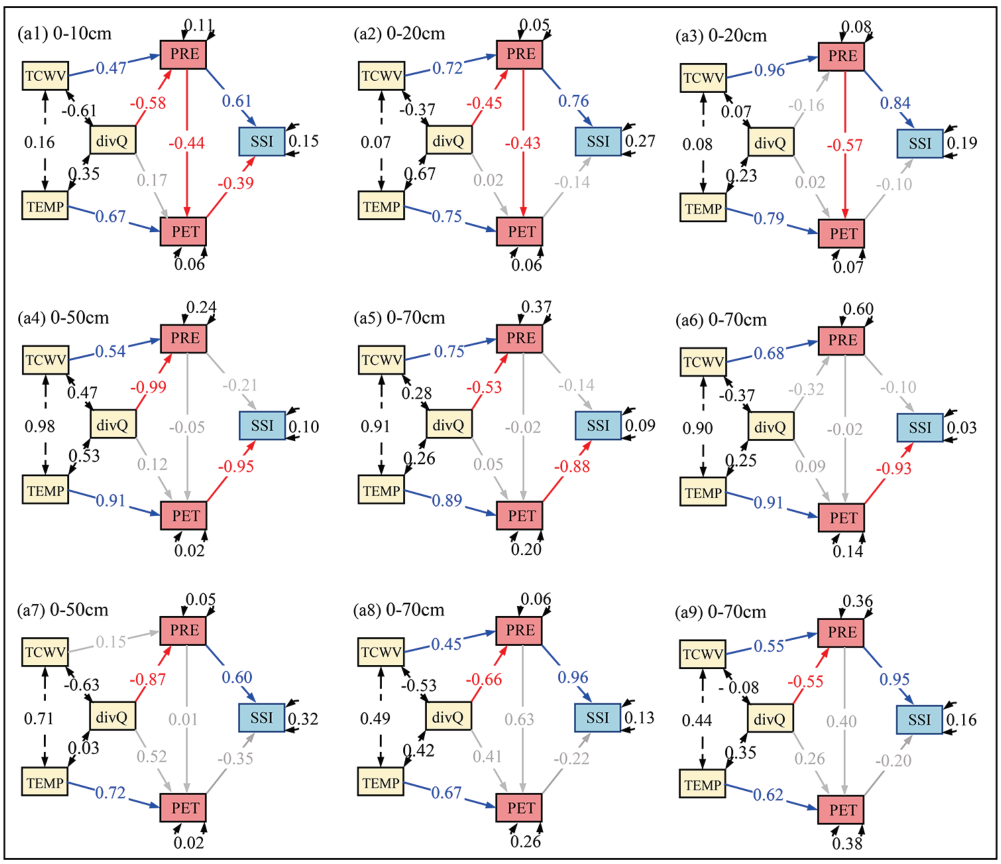

Fig.8 Path analysis of SSI in different seasons (a1, Spring 0-10cm Humid; a2, Spring 0-10cm Sub-Humid; a3, Spring 0-10cm Sub-Arid; a4, Summer 0-10cm Humid; a5, Summer 0-10cm Sub-Humid; a6, Summer 0-10cm Sub-Arid; a7, Autumn 0-10cm Humid; a8, Autumn 0-10cm Sub-Humid; a9, Autumn 0-10cm Sub-Arid)

4.3.4 Impacts change with drought severity of main factors

In Section 4.2, we find that potential evapotranspiration effects on soil moisture drought are larger in summer when soil moisture drought is more severe. To further compare the relative influence of precipitation and potential evapotranspiration on different drought groups based on severity, the quantile regression method is used to measure the impact of different quantiles of soil moisture drought on precipitation and potential evapotranspiration from 1950 to 2021 at different depths over different regions (Fig.9). It can be seen that the parameter estimates of the same variable under various quantiles are different. On the whole, the precipitation coefficient is greater than potential evapotranspiration in absolute value for most cases. For droughts at 0-10cm and 0-20cm, the regression coefficient of precipitation ranges from 0.75 to 1.05 from 1950 to 2021, and that of potential evapotranspiration ranges from -1.0 to -0.4. For droughts at 0-50cm and 0-60 cm, the regression coefficient of precipitation ranges from 0.75 to 0.9. The regression coefficient of potential evapotranspiration ranges from -0.9 to 0.5. At different depths, the influence of precipitation on SSI increases first and then decreases at the national scale, but the influence of potential evapotranspiration on SSI decreases with the increase of quantile. The absolute value of the regression coefficient reaches the maximum at 0.1 quantiles, indicating that with the increase of soil moisture drought severity, the potential evapotranspiration effect is enhanced, which means that the potential evapotranspiration contributes relatively more to severe droughts (Fig9.a).

Fig9.b shows the changes in the regression coefficients of precipitation and potential evapotranspiration in different quantiles of drought corresponding to different zones [taking the quantile regression method for 0-10 cm soil moisture drought as an example]. The regression coefficients of potential evapotranspiration in different zones show similar changes to that in the whole country, and the absolute values increase with the severity of soil drought. The change in the regression coefficient of precipitation in different regions does not show a definite trend. The effects on other soil depths' drought are similar to that on 0-10cm (Fig.S4). This suggests that potential evapotranspiration is a better indicator of soil moisture drought severity than precipitation.

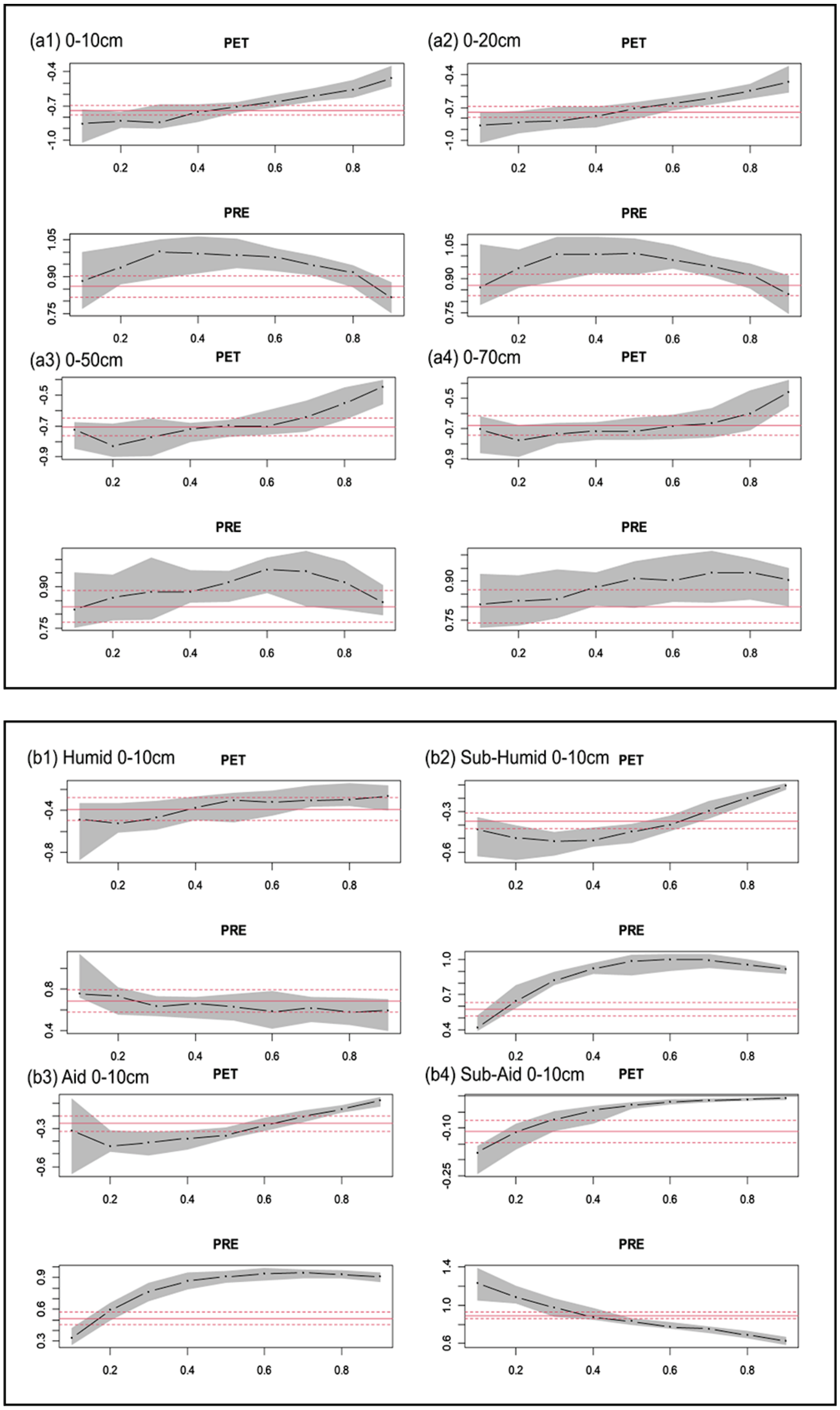

Fig.9 Changes of potential evapotranspiration and precipitation quantile regression coefficients at different depths (a) and different regions (b, 0-10cm)

5. Discussions

5.1 Soil moisture drought at different depths

Soil moisture drought determines the available water resources for crop growth and influences agricultural production. The root depth of plants increases during the growing seasons, thus enlarging the main soil moisture depth and extent where plants can extract water (Cao et al., 2019). The reductions in soil moisture are typically associated with water stress for vegetation. In this study, soil moisture droughts at four different depths (0-10cm, 0-20cm, 0-50cm, and 0-70cm) were analyzed by a three-dimensional drought identification method. We found that the duration of drought in deep layer was higher than that of soil moisture drought in surface layer, this was related to the length of time that soil water existed in different water layer depths (Xu et al., 2021). With the increase of soil layer depth, the total number of drought counts decreases. These findings demonstrate that significant variation exists among different soil moisture drought at different depths. They help us to understand the characteristics and mechanisms of droughts at different development stages and provide a reference for the future analysis of soil depth selection of different agricultural droughts.

5.2 Response patterns of soil moisture drought

The path analysis model was used to quantify the response of SSI to the changes in atmospheric water vapor movement (TCWV, divQ), temperature, precipitation, and potential evapotranspiration. TCWV, divQ, and temperature were considered to be extrinsic climatic forcing factors, while precipitation and potential evapotranspiration were considered to be the most direct factors affecting soil moisture drought. Other factors such as relative humidity and wind speed were also used in existing studies to explain the change in soil moisture drought (Karimi et al., 2020; Trnka et al., 2015). The use of relative humidity, wind speed, precipitation minus evapotranspiration, and atmosphere net inflow moisture flux in the path analysis models were also tested in this study. We found these variables bring limited improvement in the ability of the path model in terms of the variance explanation rate of the soil moisture drought. This is expected, since these variables indirectly affect soil moisture by influencing precipitation and potential evapotranspiration, and they have high similarity with the selected factors in our study. Moreover, the use of a more complex path model would bring larger uncertainty in the results. In this study, precipitation and potential evapotranspiration explained more than 50% of SSI at different soil depths, in different seasons and regions. Thus, it is quite feasible to select them as the main factors affecting SSI (Table.S1).

Generally, the path analysis model proposed in this study in investigating climate effects on soil moisture drought performed reasonably well for both the surface and deep soil layers, in different regions, although the climate effects were mostly larger for the surface than for the deep layers, and in the humid areas than in the arid areas. This is expected, since the climate effect on soil is a top-down process (Jobbagy and Jackson, 2000). The surface soil moisture is more related to the change in climate factors, while the deep soil moisture tends to have a thermal lag effect on climate factors change. In addition, the climate effects on soil moisture drought in humid areas being more significant than that in arid areas are also expected, since the land-atmosphere interaction is more obvious in humid areas than in arid areas in the process of soil moisture drought (REF). In the arid areas, in the process periods of soil moisture drought, the soil moisture will be too dry to evaporate, and the evapotranspiration would be too weak to affect the atmospheric water vapor, which will confine the land-atmosphere water circulation (Gao et al., 2019; Zeng and Yuan, 2018). The land-atmosphere coupling over humid areas can be also strong during relatively dry periods.

5.3 Increasing effect of potential evapotranspiration on soil moisture drought

Both the negative anomaly of precipitation and the positive anomaly of potential evapotranspiration have extensive effects on soil moisture drought. Precipitation has been found to play a major role in drought (Fig.9). However, under the context of global warming and changing water demand in the atmosphere, the importance of potential evapotranspiration in drought cannot be ignored (Dai, 2013). In this study, we found that there were different trends in the effect of the deficiency of precipitation on soil moisture drought with the drought severity in different regions and at different depths (Fig.9). It indicated that the impact of precipitation on drought does not show an obvious increase or decrease pattern. We also found that the effect of potential evapotranspiration on drought increases with increasing drought severity (Fig.8 and Fig.9), and these results cannot be found in previous studies using the conventional linear regression analysis. Further, potential evapotranspiration is mainly dominated by temperature in most cases when drought occurred, and temperature could explain 70% or more of the change of potential evapotranspiration in many cases. The temperature is also higher in the period of severe drought (Fig.S5) and the effect of temperature on drought decreased with the increase of soil moisture drought severity. The increase in temperature further aggravates the increase of potential evapotranspiration, promotes soil evapotranspiration, and aggravates soil moisture drought (Miralles et al., 2014; Yin et al., 2014). In other words, the high-temperature situation increases the potential evapotranspiration and the atmosphere needs more water from the soil to reach saturation, further aggravating the soil moisture drought. Meanwhile, the continuous reduction of soil moisture and limited water vapor available for evaporation have weakened land-atmosphere interaction and water cycle processes. The reduction of water vapor in the atmosphere inhibits precipitation further leading to a smaller contribution of precipitation. This shows that in extreme drought situations, soil drought is mainly caused by the continuous increase of potential evapotranspiration due to the increase in temperature (Wang and Yuan, 2022).

5.4 Uncertain effect of precipitation on soil moisture drought

The TCWV and divQ's proportion of explained variation in precipitation varies with regions and seasons (Fig.7 and Fig.8). Since atmospheric evaporation in humid regions is greater than that in arid regions and the air/atmosphere is more likely to saturate to form precipitation, it is therefore expected that the proportion of explained variation in precipitation decreases from the humid to arid areas. Moreover, in different seasons, summer has the lowest variance explanation rate for precipitation compared with spring and autumn. This is because the temperature is the highest in summer, and the continued warm temperature makes it difficult for air to saturate and thus hard for precipitation to form Lu et al. (2011).

The anomaly of precipitation is closely related to the dynamic evolution of water vapor structure (Guan et al., 2019; Kingston et al., 2015). In this study, the change in the impact of precipitation on SSI was regulated by TCWV and divQ. In Section 5.3, we found that the effect of TCWV on soil moisture drought decreases with the aggravation of soil moisture drought, but the effect of divQ fluctuates, which further leads to uncertainty in the effect of precipitation on soil moisture drought. By quantifying the effects of divQ and TCWV on precipitation (Fig.S6), we found that the influence of divQ gradually increases with the decrease of precipitation in different depths and regions during the dry period of soil moisture, and the change of TCWV is uncertain, which shows that the divQ can explain the precipitation better than TCWV to some extent. The definite effect of divQ and the ambiguous effect of TCWV on precipitation further enlarge the uncertainty of the effect of precipitation on soil moisture drought.

6. Conclusions

This study first identified soil moisture drought at different depths in the mainland of China from 1950 to 2021 by using a three-dimensional drought identification method, and then established a path analysis model based on atmospheric water vapor change and water vapor circulation to investigate the synergistic effects of water supply and demand on soil moisture droughts at different depths and regions. The primary conclusions are as follows:

(1) Generally, the distribution patterns of drought event severities at different depths were similar. However, with the increase of soil layer depth, the number of drought events decreased and averaged drought duration increased.

(2) Precipitation deficits due to the change of atmospheric movement dominated the interannual variation of soil moisture drought while increasing potential evapotranspiration due to the increased temperature less exacerbated drought, independent of the climatic zone and soil depth.

(3) The impact of potential evapotranspiration to drought increased with the severity of drought. The magnitude of the response of soil moisture drought to potential evapotranspiration was exacerbated by the deterioration of drought at high temperatures and was most pronounced during extreme drought.

(4) The precipitation and potential evapotranspiration can explain more than 50% of the change of soil moisture drought, among which the explanation proportion of precipitation is larger than that of the potential evapotranspiration. The total explanation proportion decreased continuously with increasing soil depth, and the response of shallow soil drought to changes in climate factors was greater than that of the deep drought.

(5) From the spatial perspective, the climate effects on soil moisture drought in humid areas are more significant than that in arid areas. At the temporal scale, precipitation plays the dominant role in soil moisture drought at the spring and autumn while potential evapotranspiration dominates soil moisture drought in summer.

Data availability statement

Data used in this study may be accessed in the following databases:

ERA5 reanalysis data are freely downloaded from the Copernicus Climate Change Service (C3S) Climate Date Store through the CDS API client for data access.

In situ soil moisture data can be downloaded from the National Meteorological Information Center of China (CMA) (http://cdc.cma.gov.cn/home.do).

Declaration of Competing Interest

The authors declare that they have no known competing financial interests or personal relationships that could have appeared to influence the work reported in this paper.

Acknowledgments

This work was partially supported by the Hubei Provincial Natural Science Foundation of China (Grant No. 2020CFA100), the National Natural Science Foundation of China (Grant No. 52079093) and the Overseas Expertise Introduction Project for Discipline Innovation (111 Project) (Grant No. B18037). We also thank ECMWF for the ERA5 datasets and National Meteorological Information Center of China for in situ soil moisture datasets.

Reference

A, Y.L. et al., 2019. Vertical variations of soil water and its controlling factors based on the structural equation model in a semi-arid grassland. Sci Total Environ, 691: 1016-1026. https://doi.org/10.1016/j.scitotenv.2019.07.181.

Afshar, M.H., Bulut, B., Duzenli, E., Amjad, M., Yilmaz, M.T., 2022. Global spatiotemporal consistency between meteorological and soil moisture drought indices. Agr Forest Meteorol, 316. https://doi.org/10.1016/j.agrformet.2022.108848.

An, R. et al., 2016. Validation of the ESA CCI soil moisture product in China. Int J Appl Earth Obs, 48: 28-36. https://doi.org/10.1016/j.jag.2015.09.009.

Andreadis, K.M., Clark, E.A., Wood, A.W., Hamlet, A.F., Lettenmaier, D.P., 2005. Twentieth-century drought in the conterminous United States. J Hydrometeorol, 6(6): 985-1001. https://doi.org/10.1175/Jhm450.1.

Bai, W.K., Chen, X.H., Tang, Y.H., He, Y.H., Zheng, Y.H., 2019. Temporal and spatial changes of soil moisture and its response to temperature and precipitation over the Tibetan Plateau. Hydrolog Sci J, 64(11): 1370-1384. https://doi.org/10.1080/02626667.2019.1632459.

Bennett, R., Vijaygopal, R., Kottasz, R., 2020. Willingness of people who are blind to accept autonomous vehicles: An empirical investigation. Transport Res F-Traf, 69: 13-27. https://doi.org/10.1016/j.trf.2019.12.012.

Cai, S.H. et al., 2021. Spatiotemporal characteristics of agricultural droughts based on soil moisture data in Inner Mongolia from 1981 to 2019. J Hydrol, 603. https://doi.org/10.1016/j.jhydrol.2021.127104.

Cao, Y.J. et al., 2019. An Agricultural Drought Index for Assessing Droughts Using a Water Balance Method: A Case Study in Jilin Province, Northeast China. Remote Sens-Basel, 11(9). https://doi.org/ARTN 1066

Chen, X.H., Gong, X.M., Li, D.Y., Zhang, J.P., 2019. Can information and communication technology reduce CO2 emission? A quantile regression analysis. Environ Sci Pollut R, 26(32): 32977-32992. https://doi.org/10.1007/s11356-019-06380-8.

Cheng, S.J., Huang, J.P., 2016. Enhanced soil moisture drying in transitional regions under a warming climate. J Geophys Res-Atmos, 121(6): 2542-2555. https://doi.org/10.1002/2015jd024559

Dai, A.G., 2013. Increasing drought under global warming in observations and models (vol 3, pg 52, 2013). Nat Clim Change, 3(2): 171-171. https://doi.org/10.1038/Nclimate1811.

Deng, S.S., Liu, S.X., Mo, X.G., 2021. Assessment and attribution of China's droughts using an integrated drought index derived from GRACE and GRACE-FO data. J Hydrol, 603. https://doi.org/10.1016/j.jhydrol.2021.127170.

Devlieger, I., Rosseel, Y., 2017. Factor Score Path Analysis An Alternative for SEM? Methodology-Eur, 13: 31-38. https://doi.org/10.1027/1614-2241/a000130.

Ebrahimi, E., Bayat, H., Fallah, M., 2021. Relationship of soil moisture characteristic curve and mechanical properties in Entisols and Inceptisols of Iran. Geoderma Reg, 27. https://doi.org/10.1016/j.geodrs.2021.e00434.

Gao, C.J. et al., 2019. Land-atmosphere interaction over the Indo-China Peninsula during spring and its effect on the following summer climate over the Yangtze River basin. Clim Dynam, 53(9-10): 6181-6198. https://doi.org/10.1007/s00382-019-04922-x.

Gu, L. et al., 2020a. Projected increases in magnitude and socioeconomic exposure of global droughts in 1.5 and 2 degrees C warmer climates. Hydrol Earth Syst Sc, 24(1): 451-472. https://doi.org/10.5194/hess-24-451-2020.

Gu, L., Chen, J., Yin, J.B., Xu, C.Y., Chen, H., 2020b. Drought hazard transferability from meteorological to hydrological propagation. J Hydrol, 585. https://doi.org/10.1016/j.jhydrol.2020.124761.

Guan, X.F., Yang, L.M., Zhang, Y.X., Li, J.G., 2019. Spatial distribution, temporal variation, and transport characteristics of atmospheric water vapor over Central Asia and the arid region of China. Global Planet Change, 172: 159-178. https://doi.org/10.1016/j.gloplacha.2018.06.007.

Gui, S.S., Wu, C.Y., Qu, Y., Guo, L.L., 2017. Path analysis of factors impacting China's CO2 emission intensity: Viewpoint on energy. Energ Policy, 109: 650-658. https://doi.org/10.1016/j.enpol.2017.07.034.

He, H. et al., 2022. Diagnosing anomalous characteristics of atmospheric water cycle structure during seasonal-scale drought events: A case study in middle and lower reaches of Yangtze River. Water Sci Eng, 15(2): 103-113. https://doi.org/10.1016/j.wse.2022.01.001.

Heim, R.R., 2002. A review of twentieth-century drought indices used in the United States. B Am Meteorol Soc, 83(8): 1149-1165. https://doi.org/Doi 10.1175/1520-0477-83.8.1149.

Hong, M., Lee, S.H., Lee, S.J., Choi, J.Y., 2021. Application of high-resolution meteorological data from NCAM-WRF to characterize agricultural drought in small-scale farmlands based on soil moisture deficit. Agr Water Manage, 243. https://doi.org/10.1016/j.agwat.2020.106494.

Hou, E.Q. et al., 2018. Effects of climate on soil phosphorus cycle and availability in natural terrestrial ecosystems. Global Change Biol, 24(8): 3344-3356. https://doi.org/10.1111/gcb.14093.

Huang, J.P., Wang, T.H., Wang, W.C., Li, Z.Q., Yan, H.R., 2014. Climate effects of dust aerosols over East Asian arid and semiarid regions. J Geophys Res-Atmos, 119(19): 11398-11416. https://doi.org/10.1002/2014jd021796.

Jobbagy, E.G., Jackson, R.B., 2000. Global controls of forest line elevation in the northern and southern hemispheres. Global Ecol Biogeogr, 9(3): 253-268. https://doi.org/10.1046/j.1365-2699.2000.00162.x.

Karimi, M. et al., 2020. Recent trends in atmospheric evaporative demand in Southwest Iran: implications for change in drought severity. Theor Appl Climatol, 142(3-4): 945-958. https://doi.org/10.1007/s00704-020-03349-3.

Keller, A.B. et al., 2022. Soil carbon stocks in temperate grasslands differ strongly across sites but are insensitive to decade-long fertilization. Global Change Biol, 28(4): 1659-1677. https://doi.org/10.1111/gcb.15988.

Kingston, D.G., Stagge, J.H., Tallaksen, L.M., Hannah, D.M., 2015. European-Scale Drought: Understanding Connections between Atmospheric Circulation and Meteorological Drought

Indices. J Climate, 28(2): 505-516. https://doi.org/10.1175/Jcli-D-14-00001.1.

Koenker, R., Bassett, G., 1978. Regression Quantiles. Econometrica, 46(1): 33-50. https://doi.org/10.2307/1913643.

Kreibich, H. et al., 2022. The challenge of unprecedented floods and droughts in risk management. Nature, 608(7921): 80-86. https://doi.org/10.1038/s41586-022-04917-5.

Li, H.Q., Ye, A.Z., Zhang, Y.H., Zhao, W.W., 2021. InterComparison and Evaluation of MultiSource Soil Moisture Products in China. Earth Space Sci, 8(10). https://doi.org/10.1029/2021EA001845.

Ling, X.L. et al., 2021. Comprehensive evaluation of satellite-based and reanalysis soil moisture products using in situ observations over China. Hydrol Earth Syst Sc, 25(7): 4209-4229. https://doi.org/10.5194/hess-25-4209-2021.

Liu, C., Huang, W., Feng, S., Chen, J.H., Zhou, A.F., 2018. Spatiotemporal variations of aridity in China during 1961-2015: decomposition and attribution. Sci Bull, 63(18): 1187-1199. https://doi.org/10.1016/j.scib.2018.07.007.

Liu, S.P. et al., 2017. Risk factors for postpartum depression among Chinese women: path model analysis. Bmc Pregnancy Childb, 17. https://doi.org/10.1186/s12884-017-1320-x.

Liu, Y. et al., 2019. Understanding the Spatiotemporal Links Between Meteorological and Hydrological Droughts From a Three-Dimensional Perspective. J Geophys Res-Atmos, 124(6): 3090-3109. https://doi.org/10.1029/2018jd028947

Liu, Y.W., Liu, Y.B., Wang, W., Fan, X.W., Cui, W., 2022. Soil moisture droughts in East Africa: Spatiotemporal patterns and climate drivers. J Hydrol-Reg Stud, 40. https://doi.org/10.1016/j.ejrh.2022.101013.

Lloyd-Hughes, B., 2012. A spatio-temporal structure-based approach to drought characterisation. Int J Climatol, 32(3): 406-418. https://doi.org/10.1002/joc.2280.

Lu, E., Luo, Y.L., Zhang, R.H., Wu, Q.X., Liu, L.P., 2011. Regional atmospheric anomalies responsible for the 2009-2010 severe drought in China. J Geophys Res-Atmos, 116. https://doi.org/10.1029/2011jd015706.

Luo, L.F. et al., 2017. Contribution of temperature and precipitation anomalies to the California drought during 2012-2015. Geophys Res Lett, 44(7): 3184-3192. https://doi.org/10.1002/2016gl072027.

Manning, C. et al., 2018. Soil Moisture Drought in Europe: A Compound Event of Precipitation and Potential Evapotranspiration on Multiple Time Scales. J Hydrometeorol, 19(8): 1255-1271. https://doi.org/10.1175/Jhm-D-18-0017.1.

Miralles, D.G., Teuling, A.J., van Heerwaarden, C.C., de Arellano, J.V.G., 2014. Mega-heatwave temperatures due to combined soil desiccation and atmospheric heat accumulation. Nat Geosci, 7(5): 345-349. https://doi.org/10.1038/Ngeo2141.

Mpelasoka, F., Hennessy, K., Jones, R., Bates, B., 2008. Comparison of suitable drought indices for climate change impacts assessment over Australia towards resource management. Int J Climatol, 28(10): 1283-1292. https://doi.org/10.1002/joc.1649.

Narasimhan, B., Srinivasan, R., 2005. Development and evaluation of Soil Moisture Deficit Index (SMDI) and Evapotranspiration Deficit Index (ETDI) for agricultural drought monitoring. Agr Forest Meteorol, 133(1-4): 69-88. https://doi.org/10.1016/j.agrformet.2005.07.012.

Nemergut, D.R. et al., 2011. Global patterns in the biogeography of bacterial taxa. Environ Microbiol, 13(1): 135-144. https://doi.org/10.1111/j.1462-2920.2010.02315.x.

Rosseel, Y., 2012. lavaan: An R Package for Structural Equation Modeling. J Stat Softw, 48(2): 1-36. https://doi.org/DOI 10.18637/jss.v048.i02.

Song, X.W., Lyu, S.D., Wen, X.F., 2020. Limitation of soil moisture on the response of transpiration to vapor pressure deficit in a subtropical coniferous plantation subjected to seasonal drought. J Hydrol, 591. https://doi.org/10.1016/j.jhydrol.2020.125301.

Stefanon, M., Drobinski, P., D'Andrea, F., Lebeaupin-Brossier, C., Bastin, S., 2014. Soil moisture-temperature feedbacks at meso-scale during summer heat waves over Western Europe. Clim Dynam, 42(5-6): 1309-1324. https://doi.org/10.1007/s00382-013-1794-9.

Trnka, M. et al., 2015. Drivers of soil drying in the Czech Republic between 1961 and 2012. Int J Climatol, 35(9): 2664-2675. https://doi.org/10.1002/joc.4167.

Van Loon, A.F., 2015. Hydrological drought explained. Wires Water, 2(4): 359-392. https://doi.org/10.1002/wat2.1085.

Velayati, A., Sadatmahalleh, S.J., Ziaei, S., Kazemnejad, A., 2021. The role of personal factors in quality of life among Iranian women with vaginismus: a path analysis. Health Qual Life Out, 19(1). https://doi.org/10.1186/s12955-021-01799-5.

Viggiano, M. et al., 2021. The role of temporal resolution of meteorological inputs from reanalysis data in estimating air humidity for modelling applications. Agr Forest Meteorol, 311. https://doi.org/10.1016/j.agrformet.2021.108672.

Waldrop, M.P. et al., 2017. The interacting roles of climate, soils, and plant production on soil microbial communities at a continental scale. Ecology, 98(7): 1957-1967. https://doi.org/10.1002/ecy.1883.

Wang, A.H., Lettenmaier, D.P., Sheffield, J., 2011. Soil Moisture Drought in China, 1950-2006. J

Climate, 24(13): 3257-3271. https://doi.org/10.1175/2011jcli3733.1.

Wang, Y.M., Yuan, X., 2022. Land-atmosphere coupling speeds up flash drought onset. Sci Total Environ, 851. https://doi.org/10.1016/j.scitotenv.2022.158109.

Wang, Y.Q., Yang, J., Chen, Y.N., Wang, A.Q., De Maeyer, P., 2018. The Spatiotemporal Response of Soil Moisture to Precipitation and Temperature Changes in an Arid Region, China. Remote Sens-Basel, 10(3). https://doi.org/10.3390/rs10030468.

Wilhite, D.A., Hayes, M.J., Knutson, C., Smith, K.H., 2000. Planning for drought: Moving from crisis to risk management. J Am Water Resour As, 36(4): 697-710. https://doi.org/10.1111/j.1752-1688.2000.tb04299.x.

Wu, G.Y. et al., 2022. Impacts of Global Climate Warming on Meteorological and Hydrological Droughts and Their Propagations. Earths Future, 10(3). https://doi.org/10.1029/2021EF002542.

Wu, H.C., Yang, Q.L., Liu, J.M., Wang, G.Q., 2020. A spatiotemporal deep fusion model for merging satellite and gauge precipitation in China. J Hydrol, 584. https://doi.org/10.1016/j.jhydrol.2020.124664.

Xu, H.J., Wang, X.P., Zhao, C.Y., Zhang, X.X., 2019. Responses of ecosystem water use efficiency to meteorological drought under different biomes and drought magnitudes in northern China. Agr Forest Meteorol, 278. https://doi.org/10.1016/j.agrformet.2019.107660.

Xu, K. et al., 2015. Spatio-temporal variation of drought in China during 1961-2012: A climatic perspective. J Hydrol, 526: 253-264. https://doi.org/10.1016/j.jhydrol.2014.09.047.

Xu, Z.G., Wu, Z.Y., He, H., Guo, X., Zhang, Y.L., 2021. Comparison of soil moisture at different depths for drought monitoring based on improved soil moisture anomaly percentage index.

Water Sci Eng, 14(3): 171-183. https://doi.org/10.1016/j.wse.2021.08.008

Yan, G.X., Liu, Y., Chen, X., 2018. Evaluating satellite-based precipitation products in monitoring drought events in southwest China. Int J Remote Sens, 39(10): 3186-3214. https://doi.org/10.1080/01431161.2018.1433892.

Yang, Y.Q. et al., 2021. Evaluation of Multi-Source Soil Moisture Datasets over Central and Eastern Agricultural Area of China Using In Situ Monitoring Network. Remote Sens-Basel, 13(6). https://doi.org/10.3390/rs13061175.

Yin, D.Q., Roderick, M.L., Leech, G., Sun, F.B., Huang, Y.F., 2014. The contribution of reduction in evaporative cooling to higher surface air temperatures during drought. Geophys Res Lett, 41(22): 7891-7897. https://doi.org/10.1002/2014gl062039.

Zeng, D.W., Yuan, X., 2018. Multiscale Land-Atmosphere Coupling and Its Application in Assessing Subseasonal Forecasts over East Asia. J Hydrometeorol, 19(5): 745-760. https://doi.org/10.1175/Jhm-D-17-0215.1.

Zhang, L.Q. et al., 2022. Analysis of flash droughts in China using machine learning. Hydrol Earth Syst Sc, 26(12): 3241-3261. https://doi.org/10.5194/hess-26-3241-2022.

Zhang, N. et al., 2015. Effects of Social Support About Physical Activity on Social Networking Sites: Applying the Theory of Planned Behavior. Health Commun, 30(12): 1277-1285. https://doi.org/10.1080/10410236.2014.940669.

Zhang, R.Q. et al., 2021a. Assessment of Agricultural Drought Using Soil Water Deficit Index Based on ERA5-Land Soil Moisture Data in Four Southern Provinces of China. Agriculture-Basel, 11(5). https://doi.org/10.3390/agriculture11050411.

Zhang, Y. et al., 2021b. Agricultural drought prediction in China based on drought propagation and large-scale drivers. Agr Water Manage, 255. https://doi.org/10.1016/j.agwat.2021.107028.

Zhu, Y. et al., 2019. Three dimensional characterization of meteorological and hydrological droughts and their probabilistic links. J Hydrol, 578. https://doi.org/ARTN 124016

CRediT author statement

Jie Chen: Conceptualization, Resources, Investigation, Data Curation, Writing - Review & Editing, Supervision

Chengyun Wang: Methodology, Software, Validation, Formal analysis, Investigation, Writing - Original Draft

Lei Gu: Methodology, Software, Writing - Review & Editing

Guiyang Wu: Methodology, Software,

Shanlin Tong: Data Curation , Writing - Review & Editing

Lihua Xiong: Writing - Review & Editing

Chong-Yu Xu: Investigation, Resources, Data Curation, Writing - Review & Editing

Declaration of interests

☒The authors declare that they have no known competing financial interests or personal relationships that could have appeared to influence the work reported in this paper.

☐The authors declare the following financial interests/personal relationships which may be considered as potential competing interests:

Dear Editor,

Please find enclosed a copy of our manuscript entitled “A pathway analysis method for quantifying the contributions of precipitation and potential evapotranspiration anomalies to soil moisture drought” for potential publication in *Journal of Hydrology* as a *Research Article*.

Global climate warming, which changes the thermal and dynamic conditions of the climate system, affects the energy budget and water cycle of the land-atmosphere system, leading to more and more droughts. Soil moisture drought is one of the most important drought categories and affects plant growth or crop yields negatively. The underlying mechanism of soil moisture drought has been widely analyzed from the perspective of direct impacts, while the interactions between driving factors and soil moisture drought remain poorly understood. In this paper, we proposed a path analysis method to investigate the direct and indirect relationships between driving factors and soil moisture drought at different depths. We found that the change in atmospheric movement and temperate indirectly affected soil moisture drought through precipitation and potential evapotranspiration, and precipitation deficits dominated the interannual variation of soil moisture drought while potential evapotranspiration impacts were magnified by drought deterioration. These findings are important to analyze the synergistic effects of water supply and demand on soil moisture drought, and will be vital to understand the drought development mechanisms.

This manuscript has not been published or presented elsewhere in part or entirety, and it is not under consideration by another journal. We also declare no competing financial interests. All authors have worked on the manuscript and approved its submission to *Journal of Hydrology*.

Thank you very much for considering our manuscript.

Sincerely yours,

Prof. Jie Chen, on behalf of all authors
State Key Laboratory of Water Resources and Hydropower Engineering Science, Wuhan University, Wuhan 430072, China
Telephone:17764063119
Email: jiechen@whu.edu.cn

Fig.1

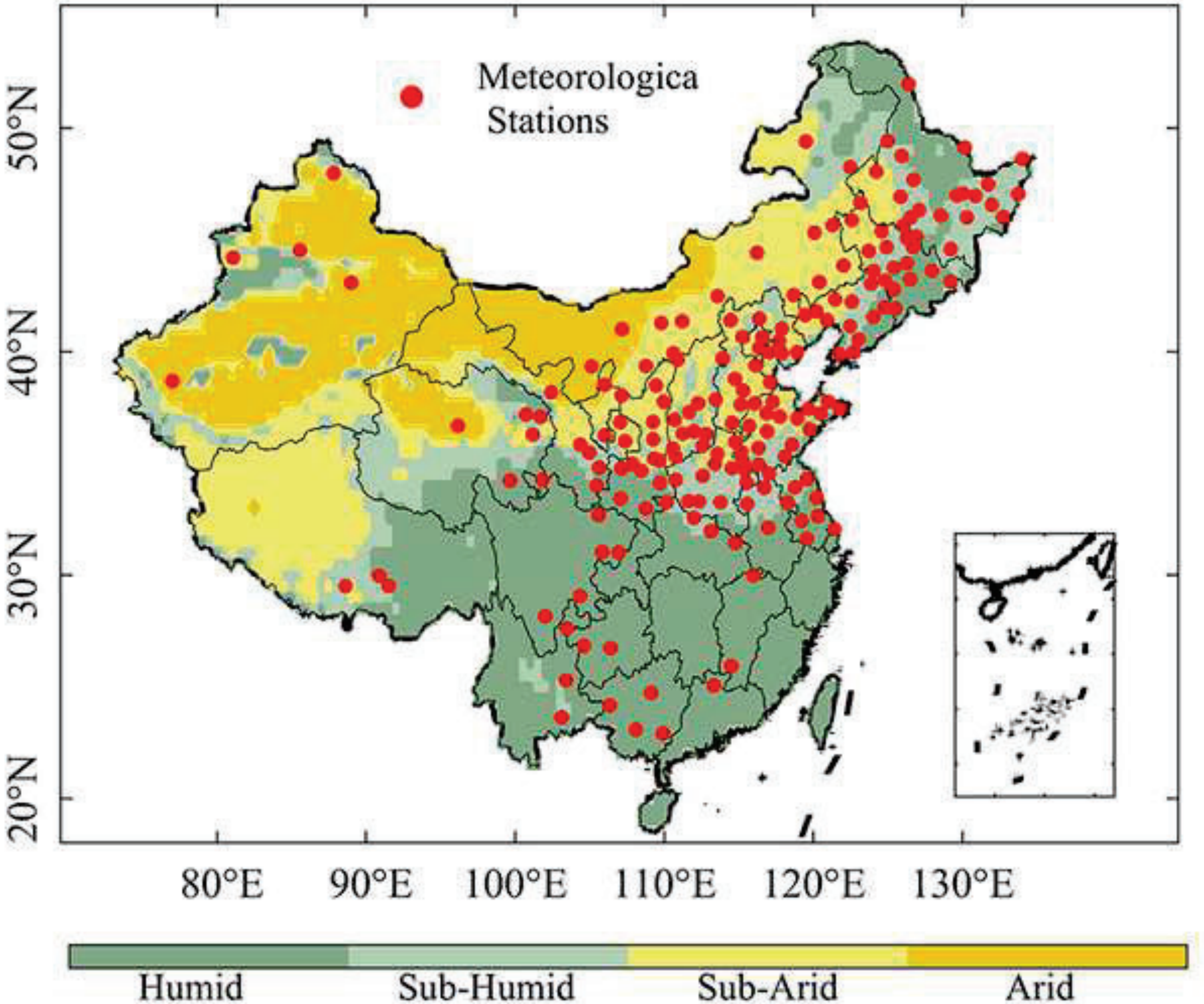

Meteorologica
Stations
50°N
40°N
30°N
20°N
80°E
90°E
100°E
110°E
120°E
130°E
Humid
Sub-Humid
Sub-Arid
Arid

Fig.2

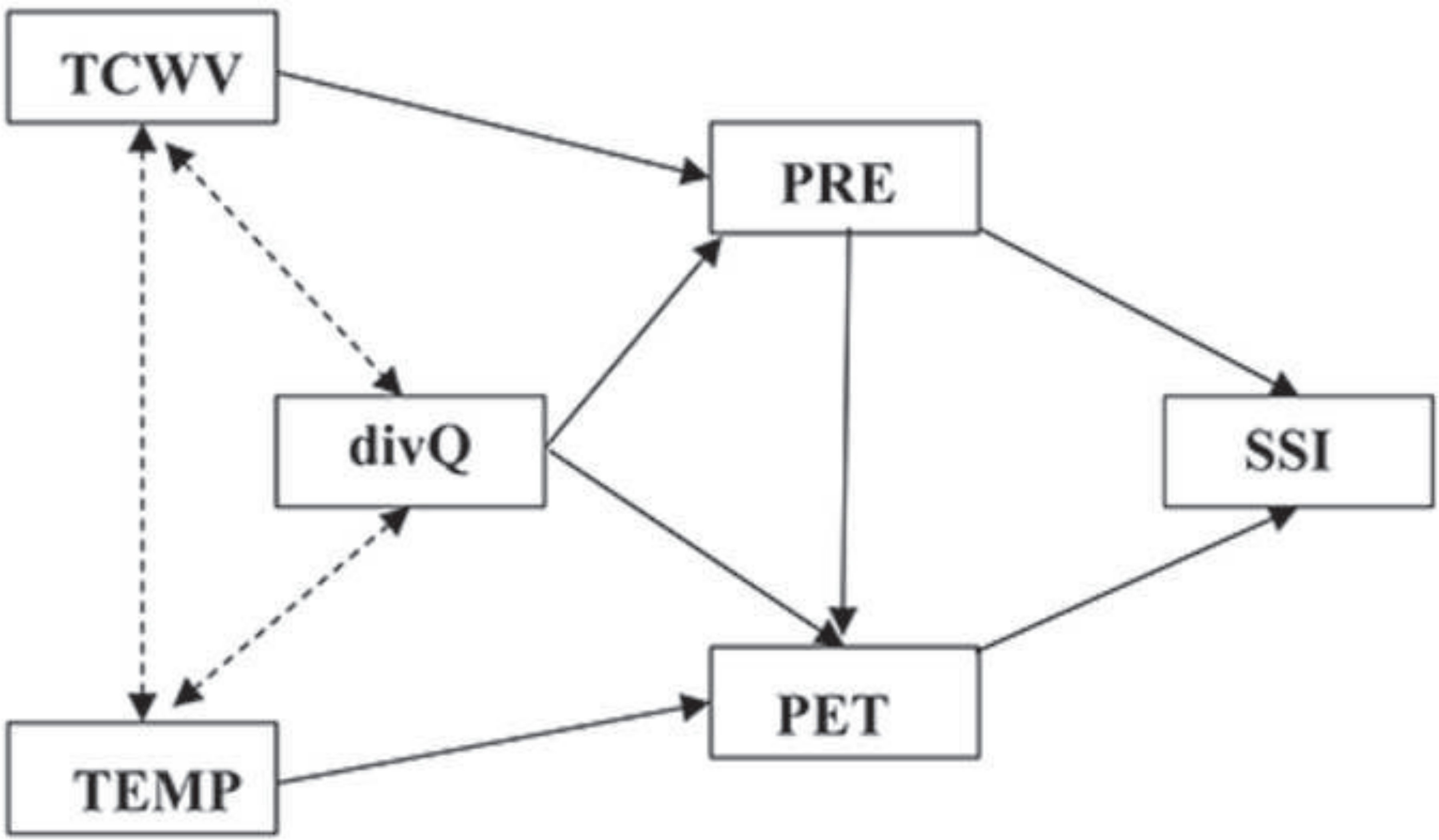

Fig.3

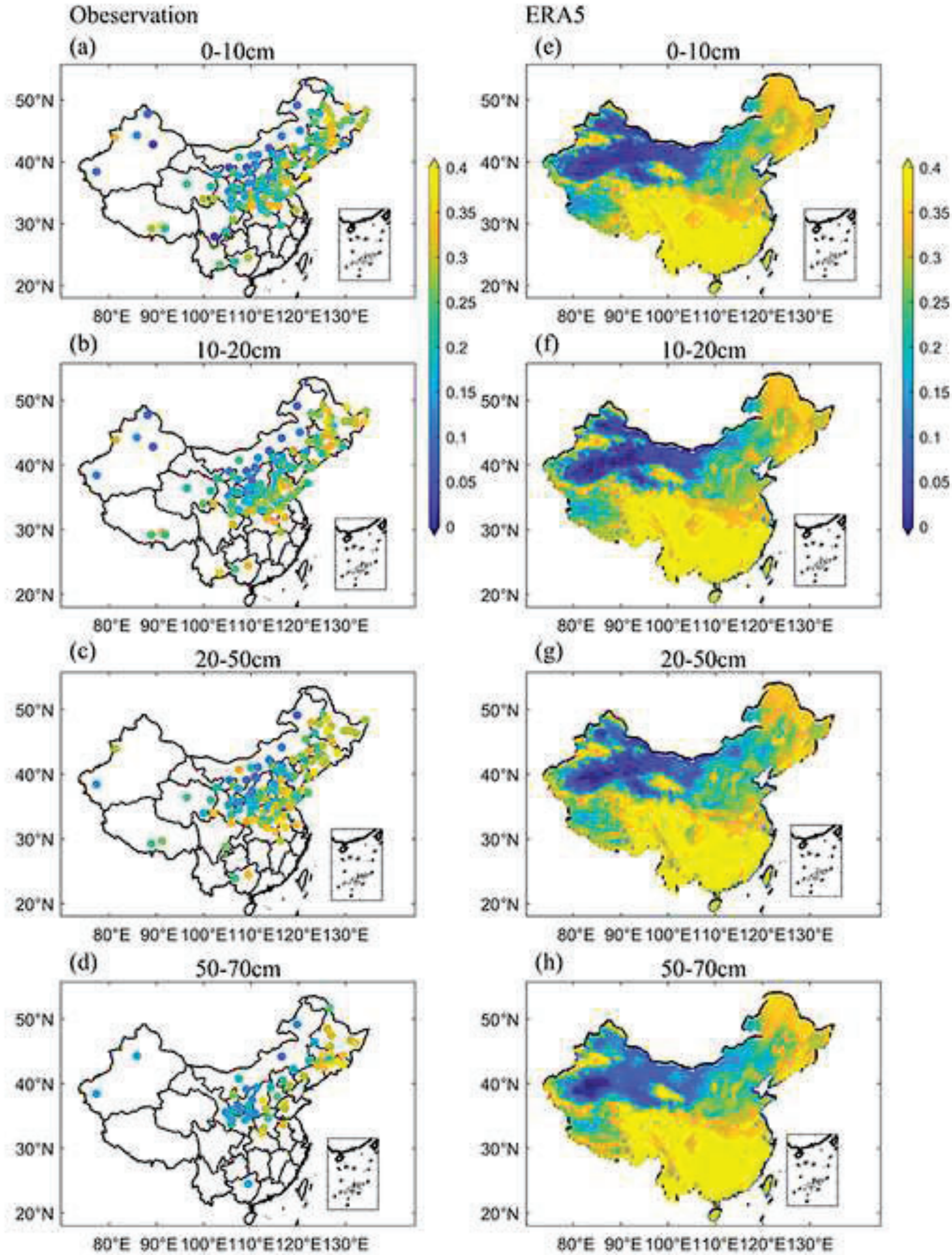

Obeservation
ERA5
(a)
0-10cm
(b)
10-20cm
(c)
20-50cm
(d)
50-70cm
(e)
0-10cm
(f)
10-20cm
(g)
20-50cm
(h)
50-70cm
50°N
40°N
30°N
20°N
80°E 90°E 100°E 110°E 120°E 130°E
0.4
0.35
0.3
0.25
0.2
0.15
0.1
0.05
0

Fig.4

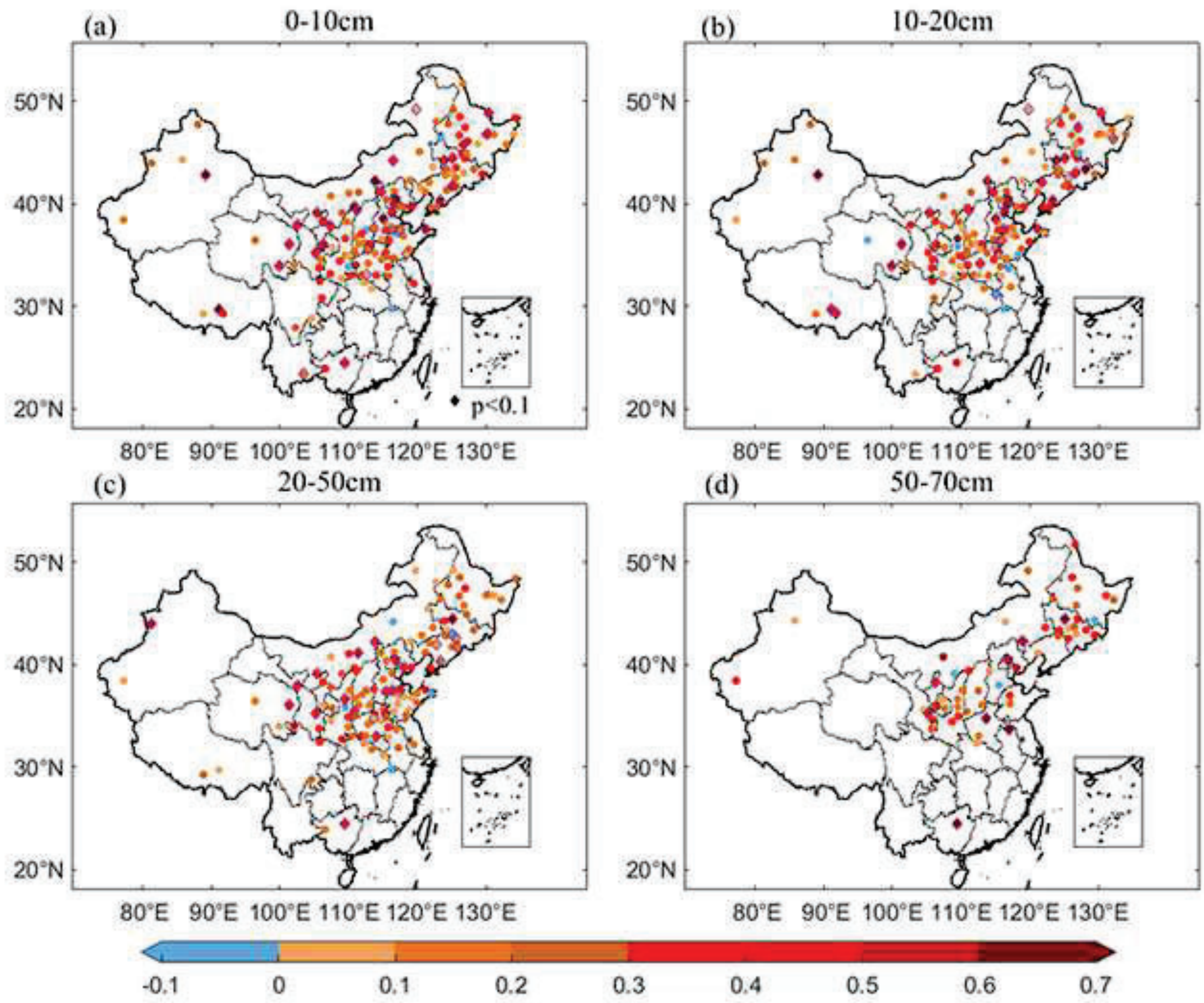
(a)
0-10cm
(b)
10-20cm
(c)
20-50cm
(d)
50-70cm
50°N
40°N
30°N
20°N
80°E 90°E 100°E 110°E 120°E 130°E
p<0.1
-0.1 0 0.1 0.2 0.3 0.4 0.5 0.6 0.7

Fig.5

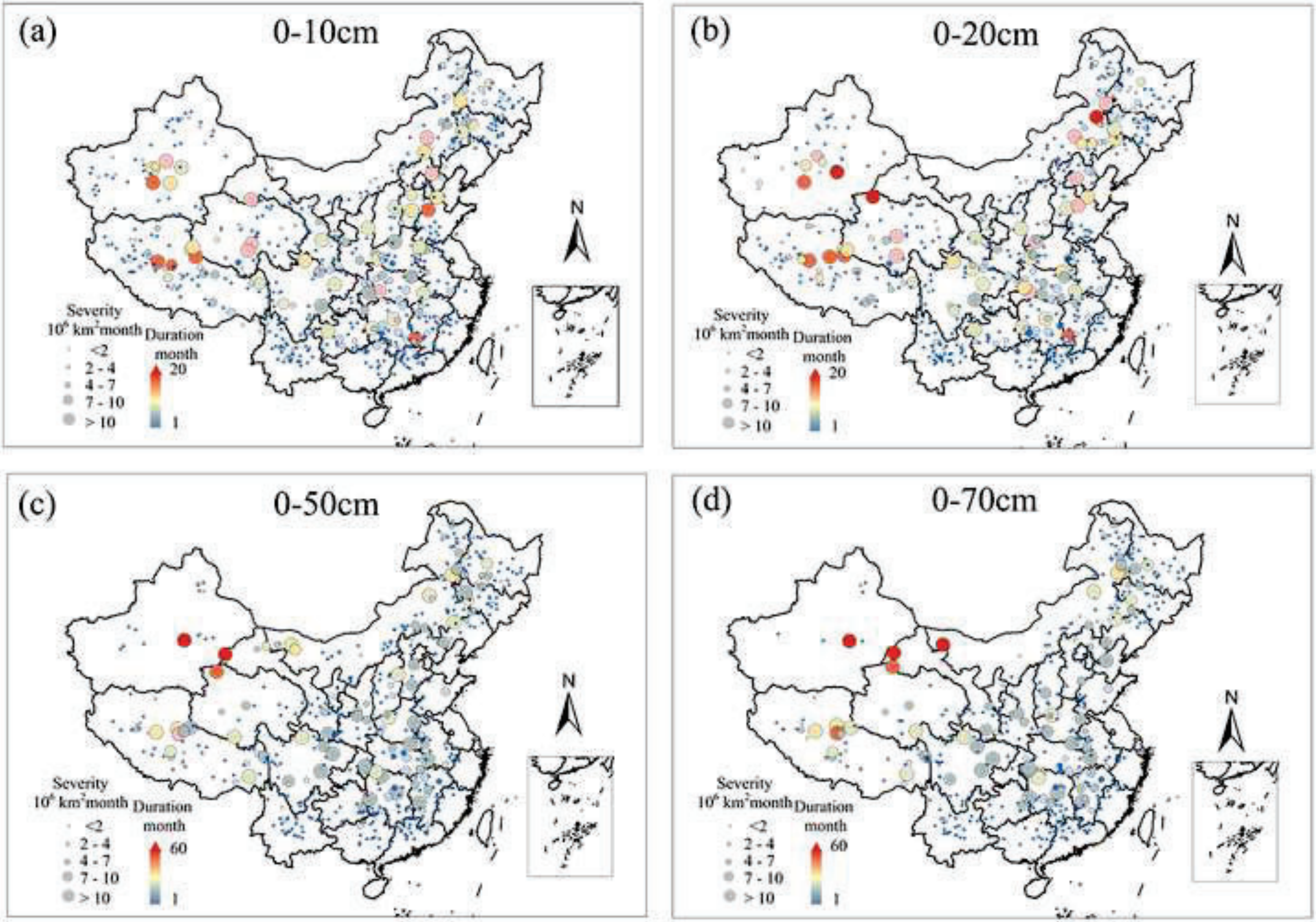
(a)
0-10cm
(b)
0-20cm
(c)
0-50cm
(d)
0-70cm
N
Severity
10^6 km^2month
<2
2 - 4
4 - 7
7 - 10
> 10
Duration
month
20
60
1

Fig.6

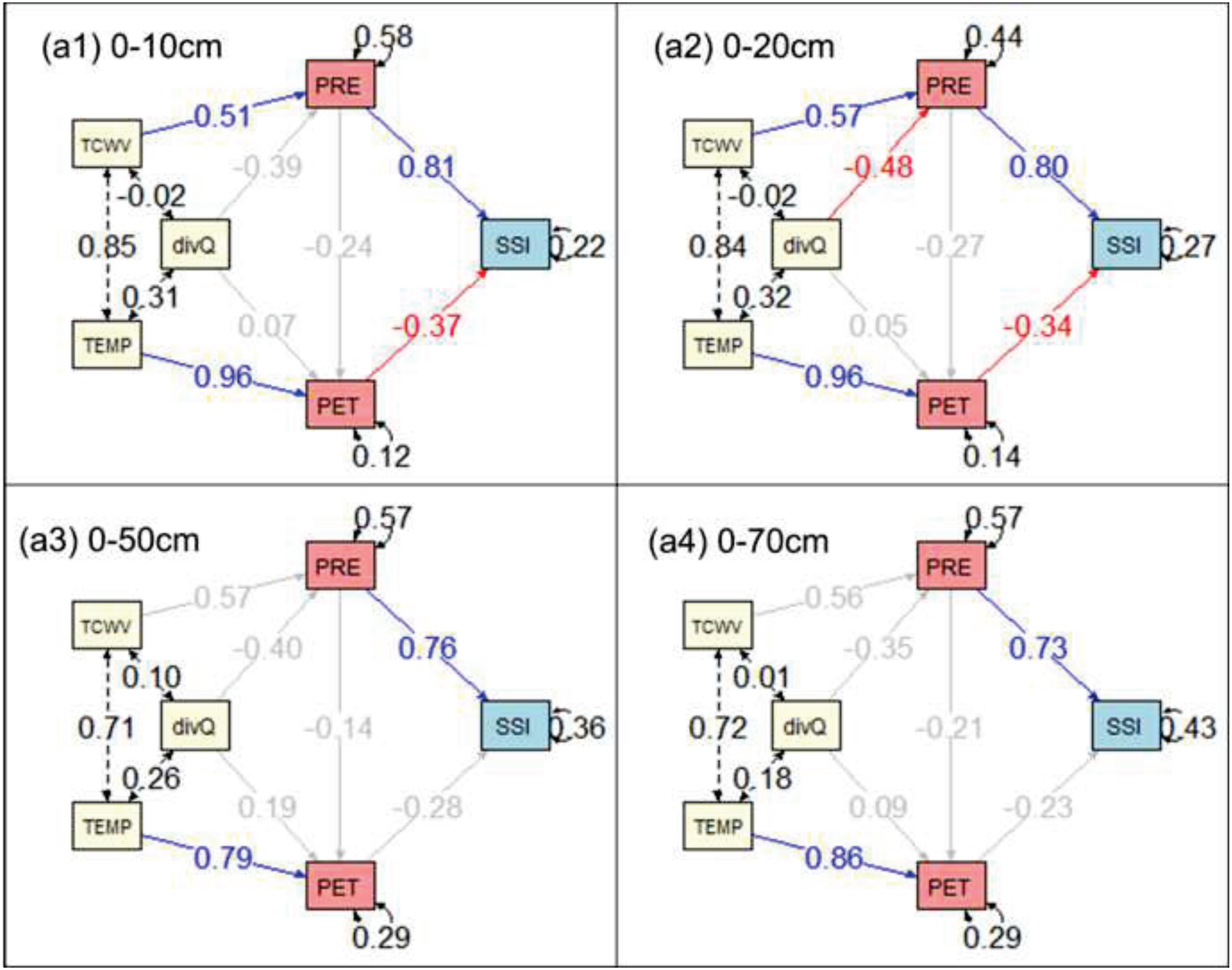

(a1) 0-10cm
PRE
PET
SSI
TCWV
divQ
TEMP
0.58
0.51
0.81
-0.39
-0.02
0.85
-0.24
0.22
0.31
0.07
-0.37
0.96
0.12
(a2) 0-20cm
PRE
PET
SSI
TCWV
divQ
TEMP
0.44
0.57
-0.48
0.80
-0.02
0.84
-0.27
0.27
0.32
0.05
-0.34
0.96
0.14
(a3) 0-50cm
PRE
PET
SSI
TCWV
divQ
TEMP
0.57
0.57
-0.40
0.76
0.10
0.71
-0.14
0.36
0.26
0.19
-0.28
0.79
0.29
(a4) 0-70cm
PRE
PET
SSI
TCWV
divQ
TEMP
0.57
0.56
-0.35
0.73
0.01
0.72
-0.21
0.43
0.18
0.09
-0.23
0.86
0.29

Fig.7

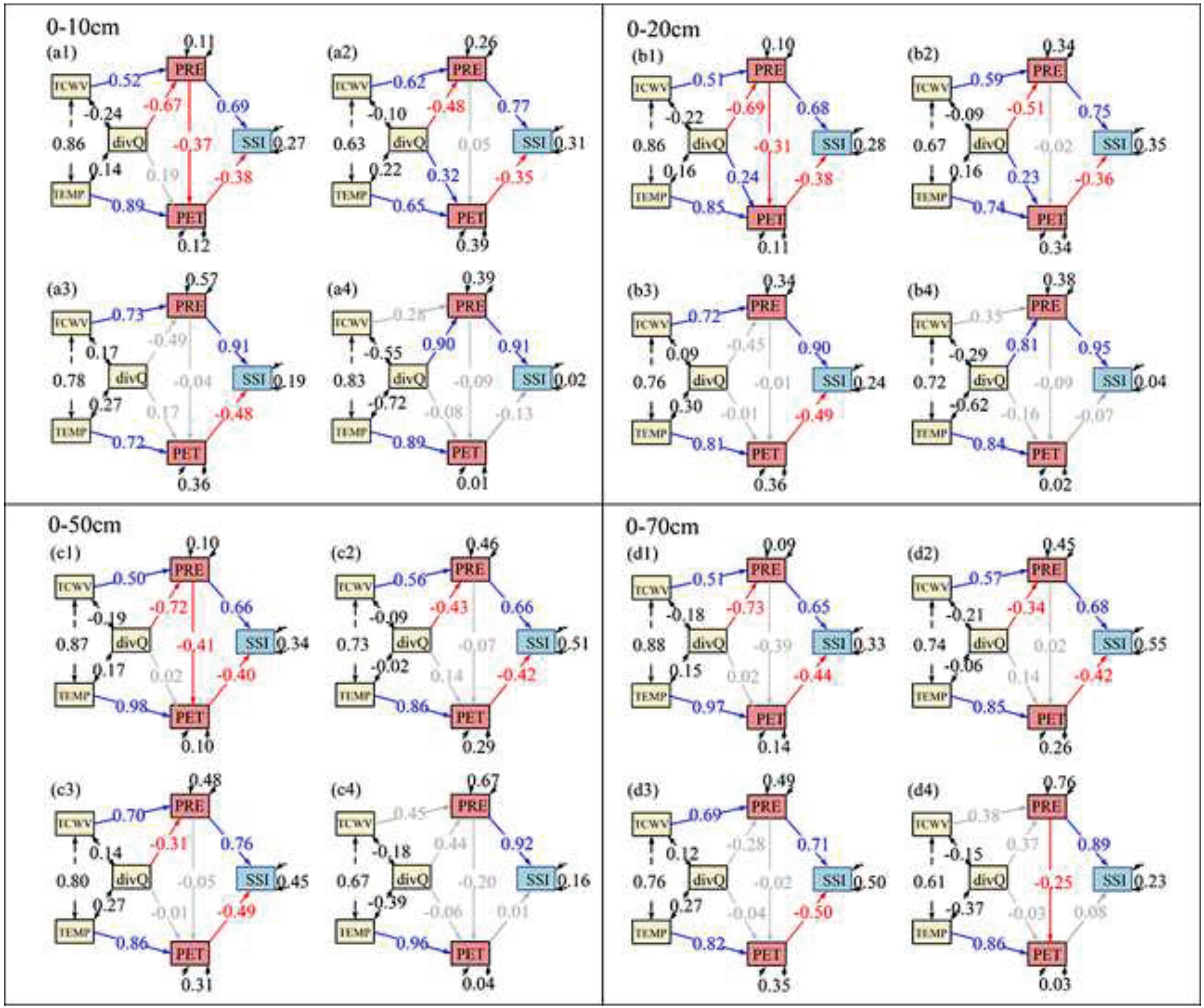
0-10cm
(a1)
(a2)
(a3)
(a4)
0-20cm
(b1)
(b2)
(b3)
(b4)
0-50cm
(c1)
(c2)
(c3)
(c4)
0-70cm
(d1)
(d2)
(d3)
(d4)
TCWV
divQ
TEMP
PRE
SSI
PET

Fig.8

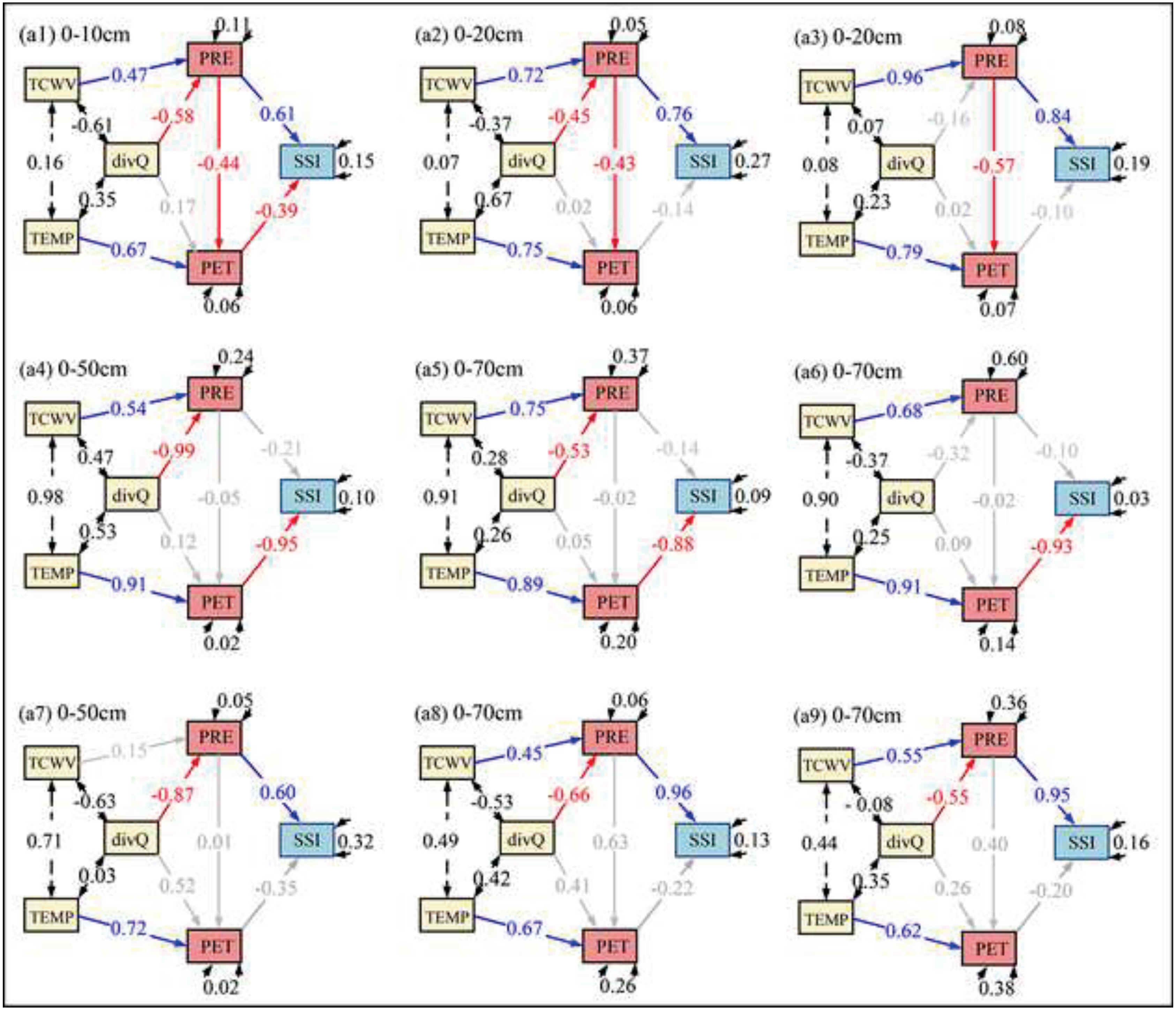
(a1) 0-10cm
TCWV PRE TEMP PET divQ SSI
0.47 0.11 -0.61 -0.58 0.61 0.16 -0.44 0.15 0.35 0.17 -0.39 0.67 0.06
(a2) 0-20cm
TCWV PRE TEMP PET divQ SSI
0.72 0.05 -0.37 -0.45 0.76 0.07 -0.43 0.27 0.67 0.02 -0.14 0.75 0.06
(a3) 0-20cm
TCWV PRE TEMP PET divQ SSI
0.96 0.08 0.07 -0.16 0.84 0.08 -0.57 0.19 0.23 0.02 -0.10 0.79 0.07
(a4) 0-50cm
TCWV PRE TEMP PET divQ SSI
0.54 0.24 0.47 -0.99 -0.21 0.98 -0.05 0.10 0.53 0.12 -0.95 0.91 0.02
(a5) 0-70cm
TCWV PRE TEMP PET divQ SSI
0.75 0.37 0.28 -0.53 -0.14 0.91 -0.02 0.09 0.26 0.05 -0.88 0.89 0.20
(a6) 0-70cm
TCWV PRE TEMP PET divQ SSI
0.68 0.60 -0.37 -0.32 -0.10 0.90 -0.02 0.03 0.25 0.09 -0.93 0.91 0.14
(a7) 0-50cm
TCWV PRE TEMP PET divQ SSI
0.15 0.05 -0.63 -0.87 0.60 0.71 0.01 0.32 0.03 0.52 -0.35 0.72 0.02
(a8) 0-70cm
TCWV PRE TEMP PET divQ SSI
0.45 0.06 -0.53 -0.66 0.96 0.49 0.63 0.13 0.42 0.41 -0.22 0.67 0.26
(a9) 0-70cm
TCWV PRE TEMP PET divQ SSI
0.55 0.36 -0.08 -0.55 0.95 0.44 0.40 0.16 0.35 0.26 -0.20 0.62 0.38

Fig.9a

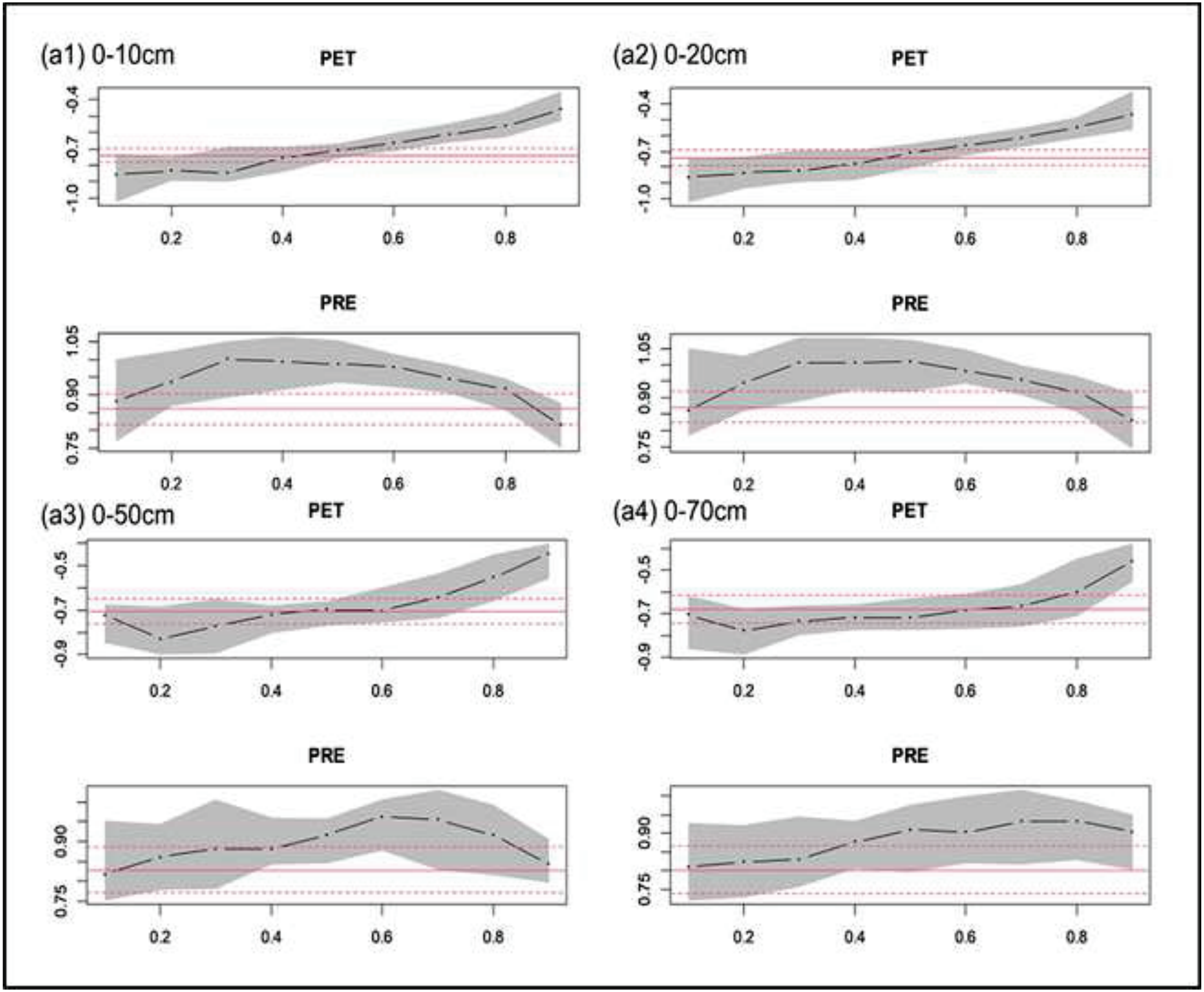
(a1) 0-10cm
PET
-0.4
-0.7
-1.0
0.2
0.4
0.6
0.8
PRE
1.05
0.90
0.75
(a2) 0-20cm
(a3) 0-50cm
-0.5
-0.7
-0.9
(a4) 0-70cm

Fig.9b

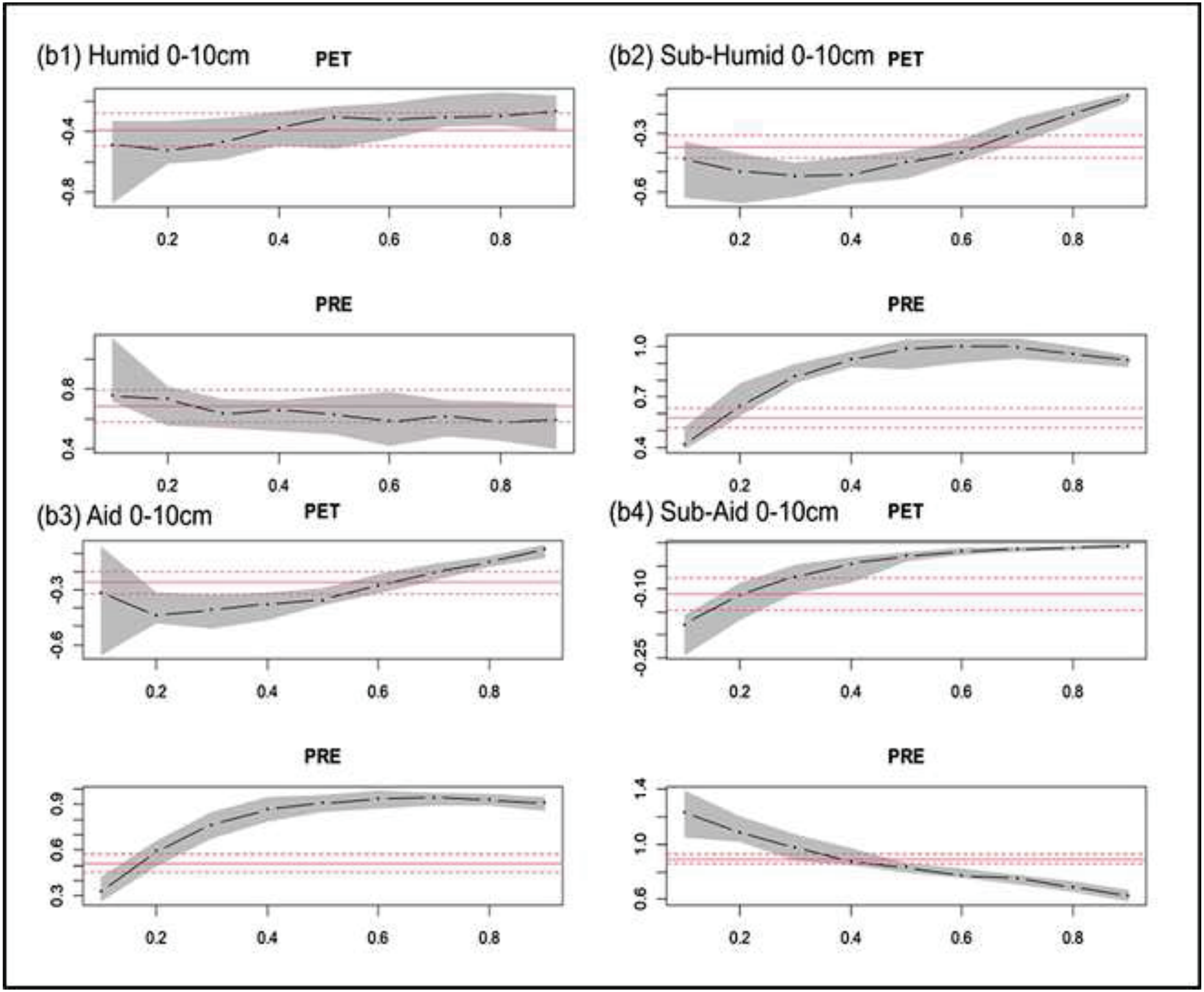
(b1) Humid 0-10cm
PET
-0.4
-0.8
0.2
0.4
0.6
0.8
PRE
0.8
0.4
(b2) Sub-Humid 0-10cm
PET
-0.3
-0.6
PRE
1.0
0.7
0.4
(b3) Aid 0-10cm
PET
-0.3
-0.6
PRE
0.9
0.6
0.3
(b4) Sub-Aid 0-10cm
PET
-0.10
-0.25
PRE
1.4
1.0
0.6

Figure 1. Distribution of soil moisture observation stations in China

Figure 2. Path diagram for SSI and possible drivers. Arrows connect exogenous and endogenous variables, called paths. The direction of the path indicated by the single-headed arrow is determined by the causal relationship between exogenous and endogenous variables. The double-headed arrow indicates a correlation between TCWV, temperature (TEMP), and divQ but not causality. TCWV, temperature, and divQ are the input variables that affect the SSI indirectly. In particular, TCWV and divQ affect SSI by affecting precipitation (PRE) and potential evapotranspiration (PET), and temperature affect SSI by affecting potential evapotranspiration, where precipitation and potential evapotranspiration directly affect the SSI.

Fig.3 Spatial distributions of annual averages of observations (a-b) and ERA5 (e-f) soil moisture at different depths (m^3m^{-3} volumetric moisture content) during JJA for the period of 1992-2011 in China

Fig.4 Correlation coefficient between ERA5 and measured soil moisture at different depths during JJA for the period of 1992-2011 in China ($P<0.1$, P means the significant level)

Fig. 5 Spatial distribution of soil moisture drought events during 1950-2021.

Fig.6 Path analysis of SSI at different depths (a1, 0-10cm; a2, 0-20cm; a3, 0-50cm; a4, 0-70cm). The arrow represents the effect path and direction, the blue and red arrows represent significant ($P<0.05$; P means the significant level) positive and negative effect paths, respectively, and the gray arrow represents the insignificant pathways. The number on the one-headed arrow is the standardized path coefficient. The black dashed doubled-headed arrow represents the simple correlation relationship between the two factors, and the number on it is the correlation coefficient.

The values on PRE, PET, and SSI are the amount of explained variation (R^2) of the variable explained by all paths in the model.

Fig.7 Path analysis of SSI in different regions (a1,0-10cm Humid; a2,0-20cm Humid; a3,0-50cm Humid; a4,0-70cm Humid; b1,0-10cm Sub-Humid; b2,0-20cm Sub-Humid; b3,0-50cm Sub-Humid; b4,0-70cm Sub-Humid; c1,0-10cm Sub-Arid; c2,0-20cm Sub-Arid; c3,0-50cm Sub-Arid; c4,0-70cm Sub-Arid; d1,0-10cm Arid; d2,0-20cm Arid; d3,0-50cm Arid; d4,0-70cm Arid)

Fig.8 Path analysis of SSI in different seasons (a1, Spring 0-10cm Humid; a2, Spring 0-10cm Sub-Humid; a3, Spring 0-10cm Sub-Arid; a4, Summer 0-10cm Humid; a5, Summer 0-10cm Sub-Humid; a6, Summer 0-10cm Sub-Arid; a7, Autumn 0-10cm Humid; a8, Autumn 0-10cm Sub-Humid; a9, Autumn 0-10cm Sub-Arid)

Fig.9 Changes of potential evapotranspiration and precipitation quantile regression coefficients at different depths (a) and different regions (b, 0-10cm)